A study on the metallicity gradients in the galactic disk using open clusters

Yogesh Chandra Joshi[1]*, Deepak[1] and Sagar Malhotra[2]

[1]Aryabhatta Research Institute of Observational Sciences, Nainital, India, [2]Indian Institute of Science Education and Research Mohali, Mohali, India

We study the metallicity distribution and evolution in the galactic disk based on the largest sample of open star clusters in the galaxy. From the catalog of 1,879 open clusters in the range of galactocentric distance (R_{GC}) from 4 to 20 kpc, we investigate the variation in metallicity in the galactic disk as functions of R_{GC}, vertical distance (Z), and ages of the clusters. In the direction perpendicular to the galactic plane, the variation in metallicity is found to follow a stepped linear relation. We estimate a vertical metallicity gradient $\frac{d[Fe/H]}{d|Z|}$ of -0.545 ± 0.046 dex kpc^{-1} for $|Z| < 0.487$ kpc and -0.075 ± 0.093 dex kpc^{-1} for $0.487 < |Z| < 1.8$ kpc. On average, metallicity variations above and below the galactic plane are found to change at similar rates. The change in metallicity in the radial direction is also found to follow a two-function linear relation. We obtain a radial metallicity gradient $\frac{d[Fe/H]}{dR_{GC}}$ of -0.070 ± 0.002 dex kpc^{-1} for $4.0 \lesssim R_{GC} \lesssim 12.8$ kpc and -0.005 ± 0.018 dex kpc^{-1} for $12.8 \lesssim R_{GC} \lesssim 20.5$ kpc, which clearly shows a strong variation in the metallicity gradient when moving from the inner to the outer galactic disk. The age−metallicity relation (AMR) is found to follow a steeper negative slope of -0.031 ± 0.006 dex Gyr^{-1} for clusters older than 240 Myr; however, there is some hint of positive metallicity age gradient for younger clusters.

KEYWORDS

galaxy, open clusters, metallicity distribution, metallicity abundance gradients, age−metallicity relation

1 Introduction

For a long time, open clusters (OCs) have been used to trace the kinematical, dynamical, and chemical evolution of the galaxy (Allen et al., 1998; Minchev et al., 2014; Bobylev et al., 2019). Since OCs span a wide range of ages and chemical compositions and mostly lie in the galactic plane, they are identified as tracers of the galactic disk (Luck et al., 2011; Toyouchi and Masashi, 2014; Joshi and Malhotra, 2023). As the ages and chemical compositions of OCs can be determined with a higher precision in comparison to the field stars, they are believed to be better tracers of the temporal and chemical evolution of the galactic properties (Netopil, 2016; Magrini et al., 2017; Donor, 2018; Spina, 2021; Zhang et al., 2021; Netopil, 2022). With over 6,000 OCs discovered in the galaxy so far, we now have a much better understanding of their properties and, as a result, of the composition of the galaxy (Joshi and Malhotra, 2023; Magrini, 2023). In recent years, the number of OCs having metallicity information has increased significantly, with large-scale spectroscopic surveys such as the Gaia-ESO Public Spectroscopic Survey (Magrini et al., 2017), GALAH (Martell et al., 2017), APOGEE (Majewski et al., 2017; Donor, 2020), and the LAMOST survey

(Zhong et al., 2020). Furthermore, due to the availability of high-quality photometric and astrometric data from the ESA Gaia mission (Gaia Collaboration et al., 2016), significant improvement has been made in the ability to refine the cluster membership, resulting in a better estimate of age and distance, among other parameters (e.g., Cantat-Gaudin, 2018; Cantat-Gaudin et al., 2020; Dias et al., 2021).

Radial abundance gradient is one of the key constraints to the galactic chemical evolution models. The exact nature of the radial metallicity gradient, reported through various tracers like planetary nebulae, HII region, OB stars, and classical Cepheids, is still not quite conclusive and portrays a diverse picture of the chemical evolution of the galaxy (e.g., Andrievsky, 2002; Daflon and Cunha, 2004; Maciel et al. 2005; Lemasle, 2008; Maciel et al. 2010; Genovali et al. 2014; da Silva, 2023, and references therein). However, having an extensive range in age, distance, and chemical composition, OCs are regarded as a better tracer than other such sources (Chen, 2008; Friel 2013; Magrini. 2023). Various studies have been carried out in the last 2 decades to study the chemical evolution of the galactic disk using OCs (e.g., Friel et al. 2002; Chen et al. 2003; Bragaglia, 2008; Friel et al. 2010; Carrera et al. 2011; Yong et al. 2012a; Frinchaboy et al. 2013a; Reddy et al. 2016; Netopil, 2016; Magrini et al. 2017). However, the main advancement came after the recent release of three large-scale surveys, namely, Gaia-ESO (Randich, 2022), GALactic Archeology with HERMES (Martell et al. 2017), and Apache Point Observatory Galactic Evolution Experiment (Majewski et al. 2017), which resulted in the estimation of more complete and precise chemical compositions of a large number of OCs (Carrera et al. 2019; Donor, 2020; Zhong et al, 2020; Spina, 2021; Zhang et al. 2021; Myers et al. 2022a; Netopil, 2022; Spina et al. 2022; Magrini, 2023). These studies have obtained a single-slope radial metallicity gradient ranging from −0.051 to −0.077 dex/kpc while employing a two-function radial metallicity gradient, and they obtained a steeper slope in the range of −0.054 to −0.081 dex/kpc for the younger and inner region of the clusters and a shallower slope of 0.009 to 0.044 dex/kpc for the older and outer region of the clusters, which is also supported by the inside-out disk formation models. The intersection point or knee point in such two-function slopes also varies between 11 and 12 kpc among different studies. The age–metallicity relation is another important constraint on the theoretical models of the galactic disk and has been studied by various authors using different stellar populations (e.g., Friel 1995; Carraro et al. 1998; Feltzing et al., 2001). Except for a few studies like Edvardsson et al. (1993), Chen et al. (2003), and Zhong et al. (2020), most of the studies found no obvious AMR for the OC population (Friel et al. 2010; Yong et al. 2012b; Netopil, 2016; Magrini et al. 2017; Zhang et al. 2021).

Considering a wide range of galactic chemical evolution parameters among different studies, the prime motive of the present work is to form a more extensive set of OCs having chemical compositions available through recent photometric and spectroscopic surveys, thus extending the sample with a wide range in the age and galactocentric distance. Despite extracting cluster parameters from different sources, hence making a heterogeneous data set, we trust that a statistical analysis on a larger sample of OCs would not lead to any systematic bias in our results. This paper is structured as follows: we describe the data used in the present work in Section 1. The metallicity distribution of OCs is analyzed in Section 2. The cluster age–metallicity relation is examined in Section 3. In Section 4, we investigate various correlations between radial and vertical metallicity gradients with the age and positions of the OCs. Our results are summarized in Section 5.

2 Data

To understand the chemical evolution of the galaxy, particularly the galactic disk, over the last few billion years, a large and homogeneous sample of OCs with measured metallicity and age is required. For this purpose, we searched the literature for OCs with known metallicity along with other information like position coordinates, radial distances, and age. It may be noted here that we have used the term metallicity for iron abundance [Fe/H] (relative to the solar abundance) throughout this study. Most of the OC metallicity estimates reported prior to 2018 are either based on photometric techniques (Kharchenko, 2013) or low-resolution spectroscopic data (e.g., Netopil, 2016, and references therein). Additionally, over the years, many of the clusters have been studied repeatedly, and thus, metallicity estimates for these clusters are available based on different techniques, spectral resolutions, and data qualities. To create a comprehensive list of OCs with the best available metallicity estimate, we started by collecting all the metallicity estimates along with other related information like the method of estimation (photometric or spectroscopic), spectral resolution, signal-to-noise ratio (SNR), number of member stars used for average metallicity estimation, and the year of reporting from all the major studies published in the last three decades. This resulted in a total of 4,772 metallicity reports for known OCs, Baratella, 2020; Bragaglia, 2008; Caetano, 2015; Carraro, 2004; Carraro G. et al., 2007; Carraro Giovanni et al., 2007; Carraro, 2008; Carrera, 2012; Carrera et al., 2015; Carrera et al., 2019; Casamiquela et al., 2019; Casamiquela et al., 2021; Claria et al., 1989; Clariá, 2003; Clariá, 2008; Conrad, 2014; D'Orazi et al., 2009; De Silva et al., 2007; De Silva, 2015; Dias et al., 2021; Donati et al., 2015a; Donor, 2018; Donor, 2020; Ford et al., 2005; Fossati, 2011; Friel and Boesgaard, 1992; Friel et al., 2002; Frinchaboy, 2004; Frinchaboy, 2013b; Fu et al., 2022; Geisler et al., 2012; Gonzalez and George, 2000; Gratton et al., 1994; Hasegawa et al., 2008; Hill et al., 1999; Jacobson et al., 2008; Jacobson and Eileen, 2013; Krisciunas et al., 2015; Luck 1994; Magrini, 2010; Magrini et al., 2018; Margheim, 2000; Monroe and Catherine, 2010; Myers, 2022b; Netopil et al., 2013; Netopil, 2016; Netopil, 2022; Overbeek et al., 2016; Pasquini et al., 2004; Paunzen et al., 2003; Paunzen, 2010; Pereira et al., 2010; Piatti et al., 1995; Randich, 2022; Reddy et al., 2013; Santos, 2009; Santos, 2012; Schuler, 2003; Sestito et al., 2003; Spina, 2021; Twarog et al., 1997; Vansevicius, 1997; Villanova et al., 2005; Warren and Cole, 2009; Yong et al., 2012a; Začs et al., 2011; Zhong et al., 2020; and the reference therein, which also includes multiple reporting from different studies for some clusters. To avoid duplication of OCs in the list because of the use of different identifiers for a cluster in different studies, we used the astroquery.simbad package to detect and assign a common name to all such duplicates. As a secondary measure, we manually searched and checked all the possible duplicates with a spatial angular distance of less than 0.1° along with a maximum difference of 5 milli-arcsec in the OC's proper motion. This helped us in detecting and eliminating five more duplicate OC pairs: Berkeley 85–Dolidze 41,

COIN-Gaia23–Majaess 65, NGC 1746–NGC 1750, vdBergh-Hagen 72–UBC 491, and vdBergh-Hagen 84–Gulliver 35. Some of the other OC pairs, like UBC 55–FSR 686 and UBC 73–Gulliver 56, have very small separations in phase space but are confirmed as different clusters in previous studies. For example, Piecka et al., 2021 suggested that UBC 55 and FSR 686 are a possible pair of binary clusters, while UBC 73 and Gulliver 56 are also different clusters.

To select the best unique metallicity estimate from multiple reporting for each of the clusters, we selected the metallicity estimates by giving higher priority to spectroscopic studies (compared to the photometric metallicity estimate), followed by the highest spectral resolution, highest SNR, highest number of member stars used to find the average metallicity for the OC, smallest error in the reported metallicity, and latest reporting. This resulted in a final sample of 1,879 unique OCs with the best available metallicity estimates, of which 615 have metallicity estimates based on spectroscopic data (hereafter sample OCS, where "S" stands for spectroscopic) and the remaining 1,264 have metallicity estimates based on the photometric data (hereafter sample OCP, where "P" stands for photometric).

Like metallicity selection, we selected the best-quality astrometric and age data for each cluster from multiple reporting by prioritizing the most recent publication. During the selection, studies that also provide measurement uncertainties were preferred. From our final sample of 1,879 unique clusters, astrometric data (including distance information) are available for all the clusters, while age is available for all but one cluster. However, uncertainty estimates in age and metallicity parameters for all the clusters could not be found; therefore, any weighted statistical analysis cannot be done in the present study.

Adopting the galactocentric distance of the Sun, $R_\odot$, as 8.15 kpc (Reid, 2019), we calculated the galactocentric distance of the cluster using the following well-known transformation relation:

$$R_{GC} = \sqrt{R_\odot^2 + (d\,cos(b))^2 - 2R_\odot\,d\,cos(l)\,cos(b)}, \qquad (1)$$

where d, l, and b are the heliocentric distance, galactic longitude, and galactic latitude, respectively. We also used the rectangular coordinate system (X, Y, and Z), which is defined as $X = dcos(b)cos(l)$, $Y = dcos(b)sin(l)$, and $Z = dsin(b)$. The most distant cluster with metallicity information is at $R_{GC} = 20.38$ kpc, and only nine OCs are seen beyond $R_{GC} = 14$ kpc. This reveals either a lack of OCs in the outer galactic disk or observational limitations to observe such clusters due to large extinction along the line of sight. Additionally, the number of OCs decreases drastically as we move farther away from the heliocenter. For example, only 22 OCs are located beyond a heliocentric distance of 5 kpc, further suggesting that the drop in OC number with a radial distance is primarily linked to the detection limits (e.g., Joshi, 2016).

3 Metallicity distributions in open clusters

The metallicity in our cluster sample ranges from approximately −0.80 to 0.60 dex except for six OCs, namely, NGC 6204, NGC 2129, Trumpler 33, Dolidze 5, NGC 6910, and FSR 932, for which

the adopted [Fe/H] based on our selection criteria are −1.05, −1.53, −1.54, −1.94, −1.96, and −2.17, respectively. For all the six clusters, the adopted metallicities are based on spectroscopic data. For NGC 6204 and Trumpler 33, metallicity estimates are adopted from Conrad (2014), which provided the metallicity estimates based on a spectral resolution of 7,500, while for NGC 2129, Dolidze 5, NGC 6910, and FSR 932, metallicity estimates are adopted from Fu et al. (2022), which provided metallicity estimates based on data from the LAMOST survey with a spectral resolution of 1,800. For NGC 2129 and NGC 6910, Zhong et al. (2020) provided independent spectroscopic metallicity estimates of −1.426 ± 0.856 and −1.97, respectively, based on data from the LAMOST survey with a spectral resolution of 1,800. For all of these six clusters, NGC 6204, NGC 2129, Trumpler 33, Dolidze 5, NGC 6910, and FSR 932, Dias et al. (2021) provided independent photometric metallicity estimates of 0.096 ± 0.004, −0.07 ± 0.01, 0.145 ± 0.016, −0.033 ± 0.033, 0.035 ± 0.008, and −0.142 ± 0.008, respectively. For NGC 6204, Netopil (2016) and Paunzen et al. (2010) also provided photometric metallicities of 0.02 and −0.14 ± 0.10, respectively. The wrong identification of cluster member stars to estimate the cluster's average metallicity appears to be one of the main reasons for the large differences between the available spectroscopic and photometric metallicities for these six clusters. Finding the exact reason for this discrepancy is beyond the scope of this study. However, considering the unexpectedly lower metallicity and the large difference when compared to available photometric estimates for these six clusters, we exclude these six clusters from further analysis in this study. The final catalog of 1,879 OCs used in this study is provided in a machine-readable format in Table 1. Among the 1,879 clusters, 609 have metallicity estimates based on spectroscopic data (sample OCS), and the remaining 1,264 have metallicity estimates based on photometric data (sample OCP).

The metallicity functions for the sample OCP, OCS, and OCs (OCP + OCS) are shown in Figure 1. For all three cases, the Gaussian distribution fits are also drawn. The OC sample has a mean metallicity of −0.018 ± 0.004 with a sample standard deviation (σ) of 0.188. The sample of OCP has a slightly higher mean metallicity with [Fe/H] = −0.021 ± 0.005 compared to the sample of OCS, which has a mean [Fe/H] = −0.099 ± 0.007. Both OCP and OCS span an almost similar range in [Fe/H] and also have similar sample standard deviations. The small but significant difference between the mean metallicity of the sample OCP and OCS may be the result of two factors: 1) systematic offsets in the photometric metallicity estimates and 2) bias in the sample selection. Because of the unavailability of photometric data for all the cases, it is not possible to directly check for the systematic offsets in the estimated metallicities. However, as sample OCP consists of photometric metallicity estimates from many studies that provide metallicity estimates based on different sets of photometric data along with theoretical isochrones, a systematic offset in all or the majority of these studies is not expected. To examine whether bias in the sample selection is the reason behind this offset, we draw the distribution of sample OCP and OCS in the X–Y plane in the heliocentric frame in the bottom panel of Figure 2. Here, the Sun is located at (X, Y) = (0, 0) where positive X points toward the galactic center (GC) and positive Y points toward the north galactic pole. The distribution readily suggests that the OCP clusters are located more toward the GC than the clusters in OCS. This is clearer from the top panel of the figure where the density

TABLE 1 Final catalog of 1,879 OCs used in this study. The entries in the spectral resolution column (Resol.) are left blank for the studies where adopted metallicities are based on photometric data.

S.N.	Cluster ID	RA	DEC	X	Y	Z	R_{GC}	log (age)	[Fe/H]	e[Fe/H]	Resol	Reference
1	ASCC 10	51.807	34.945	−525.95	237.45	−185.60	8.681	7.90	−0.024	0.018	1,800	Fu et al. (2022)
2	ASCC 101	288.408	36.377	145.43	360.67	79.86	8.013	8.10	0.004	0.008		Dias et al. (2021)
3	ASCC 103	294.031	35.735	170.63	457.26	62.16	7.993	7.90	0.115	0.024	1,800	Fu et al. (2022)
4	ASCC 105	295.540	27.402	235.80	459.86	18.83	7.928	7.99	0.046	0.024	1,800	Fu et al. (2022)
5	ASCC 106	295.286	1.494	503.30	422.53	−119.95	7.659	8.06	0.029	0.005		Dias et al. (2021)
6	ASCC 107	297.164	21.994	445.92	739.48	−28.62	7.740	7.05	0.353	0.013		Dias et al. (2021)
7	ASCC 108	298.355	39.328	286.80	1,025.76	112.52	7.931	7.91	−0.106	0.067	1,800	Fu et al. (2022)
8	ASCC 11	53.029	44.877	−729.52	412.45	−135.99	8.890	8.45	−0.360	0.015	22,500	Myers (2022b)
9	ASCC 110	300.772	33.549	529.77	1,491.24	37.78	7.765	8.79	0.140	0.024		Dias et al. (2021)
10	ASCC 111	302.960	37.544	215.04	789.73	28.95	7.974	7.90	0.080	0.008		Dias et al. (2021)
.	…	…	…	…	…	…	…	…	…	…	…	
.	…	…	…	…	…	…	…	…	…	…	…	
1879	vdBergh 92	106.186	−11.333	−793.59	−780.59	−43.40	8.978	6.75	0.025	0.007		Dias et al. (2021)

The entire table is available in the online version in a machine-readable format.

distributions of the sample OCP and OCS along X are provided. Here, the distribution for sample OCS is more negatively skewed with a skewness of −0.23, compared to sample OCP which has a skewness of −0.15, and it is understood to be due to the presence of more clusters in the anti-GC direction in sample OCS than in the sample OCP.
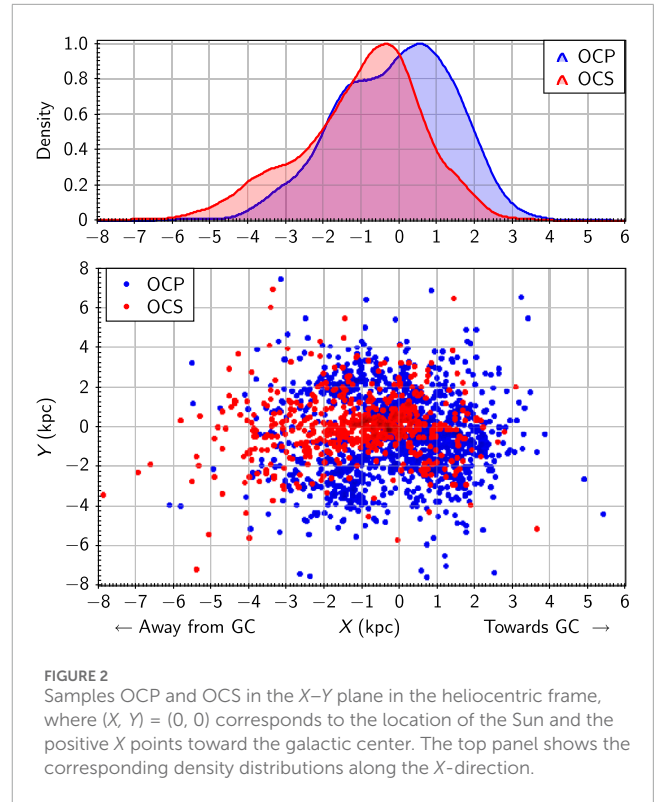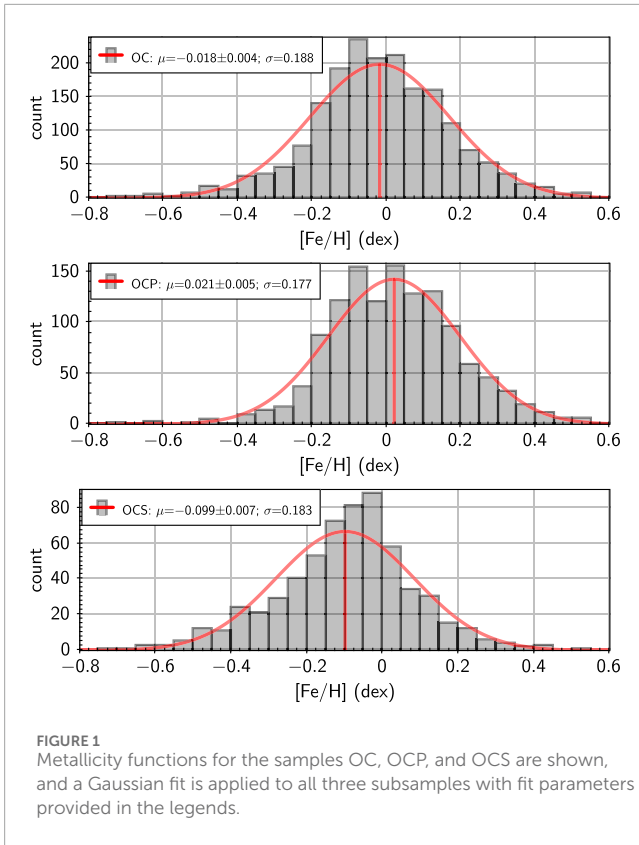
4 Age−metallicity relation

The age–metallicity relation (AMR) in the galactic disc is crucial to constrain the chemical evolution models, and star clusters offer an important advantage in the studies of the evolution of the galaxy because they provide a time sequence for investigating the changes that occur in our galaxy over the period of time. The large temporal range in the age and metallicity for the OCs provides useful insights related to the chemical evolution history of the galaxy and also presents a useful constraint on the various theoretical models of the disk (Friel 1995). Over the last 20 years, many studies that focus on this relation use either nearby stars (Carraro et al. 1998; Feltzing et al. 2001) or OCs (Netopil, 2016; Magrini et al. 2017; Döner, 2023). As noted in many earlier studies, there is no obvious AMR for the OC population (e.g., Friel et al. 2010; Yong et al. 2012b; Zhang et al. 2021), while some of the studies find a weak AMR (Edvardsson et al. 1993; Chen et al. 2003; Zhong et al. 2020). However, the large sample of OCs having metallicity measurements in the present study is re-employed to understand this relation in some detail.

The AMR in our sample of clusters is shown in Figure 3. The distribution readily suggests that for clusters with $\log(\text{age/yr}) \lessapprox 8.4$, the average metallicity of clusters is near to the solar metallicity and does not change significantly over time. However, for $\log(\text{age/yr}) \gtrapprox 8.4$, the clusters' average metallicity follows a slightly decreasing trend with an increase in $\log(\text{age/yr})$. To find the exact age–metallicity gradients and the age turn-off point at which the metallicity gradient changes, we fitted the data with a combination of two linear regressions (i.e., stepped linear regression) in the following form:

$$[\text{Fe/H}] = m_1 \times \log(\text{age/yr}) + b_1, \quad \log(\text{age/yr}) \leq C, \quad (2)$$

$$[\text{Fe/H}] = m_2 \times \log(\text{age/yr}) + b_2, \quad \log(\text{age/yr}) > C, \quad (3)$$

where C is the point of intersection, b_1 and b_2 are the [Fe/H]-axis intercepts, and m_1 and m_2 are slopes for the two functions. The coefficients of the fitted regressions (along with the point of intersection C and corresponding standard errors) were determined using iterative least square estimation by treating b_1, m_1, C, and m_2 as variables while assuming $b_2 = (m_1 \times C + b_1)$. Based on the distribution in Figure 3, we assumed the initial values of b_1, m_1, C, and m_2 as 0, 0, 8.5, and −0.02, respectively. Estimated values of coefficients from each iteration were adopted as inputs for the next iteration. Along with minimizing the mean error, we also repeated the iterations until the difference between the estimated coefficients and the corresponding adopted coefficients was less than 10^{-5}. In addition, for each of the iterations, we also checked the distribution of the fitted metallicity residual (i.e., the observed metallicity value

FIGURE 1
Metallicity functions for the samples OC, OCP, and OCS are shown, and a Gaussian fit is applied to all three subsamples with fit parameters provided in the legends.

FIGURE 2
Samples OCP and OCS in the X–Y plane in the heliocentric frame, where $(X, Y) = (0, 0)$ corresponds to the location of the Sun and the positive X points toward the galactic center. The top panel shows the corresponding density distributions along the X-direction.

minus the predicted model value) as a function of log(age/yr) and found that for the final iteration, the slope and the intercept to this distribution were less than 10^{-5}. The final fitted function to our OC data is shown as the red line in Figure 3. The coefficients of the fitted functions are also provided in the legend of Figure 3 in the following forms: b_1, m_1, C, and m_2. Based on the sample OC, the two linear functions intersect at log(age/yr) = 8.378 ± 0.093 (i.e., an age of approximately 240 Myr), and the age–metallicity gradients are given as follows:

$$\frac{d\,[\text{Fe/H}]}{d\log(\text{age/yr})} = 0.014 \pm 0.011,$$

$$\log(\text{age/yr}) \leq 8.378 \pm 0.093 \tag{4}$$

$$\frac{d\,[\text{Fe/H}]}{d\log(\text{age/yr})} = -0.159 \pm 0.021,$$

$$\log(\text{age/yr}) > 8.378 \pm 0.093 \tag{5}$$

For log(age/yr) > 8.378 ± 0.093, the decrease in [Fe/H] with an increase in log(age/yr) with a slope of $\frac{d\,[\text{Fe/H}]}{d\log(\text{age/yr})} = -0.159 \pm 0.021$ is equivalent to -0.031 ± 0.006 dex/Gyr. The negative slope between age and metallicity suggests that the metallicity in the interstellar medium of the galaxy gradually increased with time until approximately 240 Myrs ago. In Table 2, we compare our derived AMR slope with earlier studies that were carried out using OCs, although with a significantly smaller sample (Pancino, 2010; Zhong et al. 2020). Our present estimate is quite consistent with these studies. However, for log(age/yr) ≤ 8.378 ± 0.093, a very slightly increasing trend in [Fe/H] is seen with the increase in log(age/yr). Although it surprisingly suggests that the formation

site of the younger cluster is relatively metal-poor compared to the intermediate age clusters, a slope of 0.014 at almost 1-σ level is too small to make any definite conclusion. Overall, a negative slope in AMR is in agreement with the results from previous studies that the metallicity of old-age OCs is lower than that of young and intermediate-age OCs at any given galactocentric distance (e.g., Jacobson et al., 2016; Netopil, 2016; Spina, 2017). Using a homogenous compilation of 172 clusters from the literature, Netopil (2016) investigated the metallicity distribution and found that the clusters younger than 500 Myrs may be characterized by lower metallicities than the older clusters, at least in the region between 7 and 9 kpc from the GC. At the same time, they confirmed a negative gradient for these clusters. However, their sample did not include any clusters younger than 100 Myrs located in the inner galaxy.

As evident from Figure 3, the sample OCS has a relatively lower average metallicity compared to sample OCP at all the ages in the available age span. This, as discussed previously in Section 2, is possibly due to the sample selection bias as sample OCP has more clusters from the GC direction, while sample OCS has more clusters from the anti-GC direction. More interestingly, both samples have a nearly constant spread in metallicity throughout the available age span, suggesting that at both older and recent times, the natal gas at the formation site of the clusters had similar mixture properties. To understand the properties of OCs from different ages, we broadly segregate our sample OC in three different age bins, namely, ≤20 Myrs as young open clusters (YOC), 20–700 Myr as intermediate-age clusters (IOC), and > 700 Myr as old clusters (OOC). Samples YOC, IOC and OOC have 410, 1114 and 349 clusters. Metallicity functions for the sample YOC, IOC, and OOC are shown across the panels in
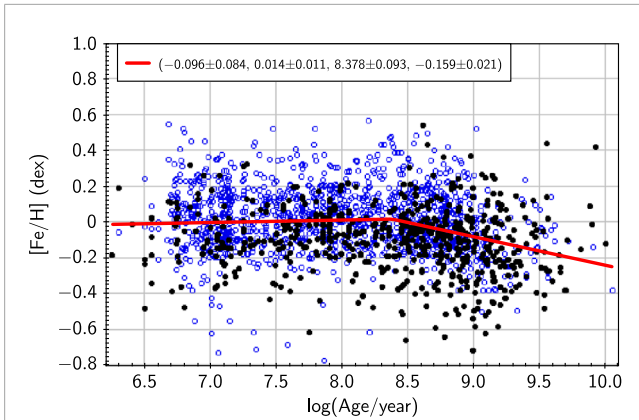
FIGURE 3
Age−metallicity functions for the sample clusters. Open blue circles and filled black circles are the clusters from the sample OCP and OCS, respectively. The red line shows the fitted stepped linear regression to the total sample, coefficients (along with corresponding standard errors) for which are provided in the legends in the forms b_1, m_1, C, and m_2, where b_1 and m_1 are the y-axis intercept and slope for the first linear function, respectively; m_2 is the slope for the second linear function; and C is the point where these two functions intersect.

TABLE 2 Comparison of the age−metallicity slope among different studies based on open clusters. The number of clusters (N) used in each study is provided in the second column.

Slope (dex Gyr^{-1})	N	Reference
−0.026	57	Pancino (2010)
−0.022 ± 0.0008	295	Zhong et al. (2020)
−0.031 ± 0.006	786	This work

TABLE 3 Comparison of vertical metallicity gradient $\left(\frac{d[Fe/H]}{d|Z|} \right)$ reported in the previous studies with estimates in this work. The number of clusters (N) used in each study is provided in the third column.
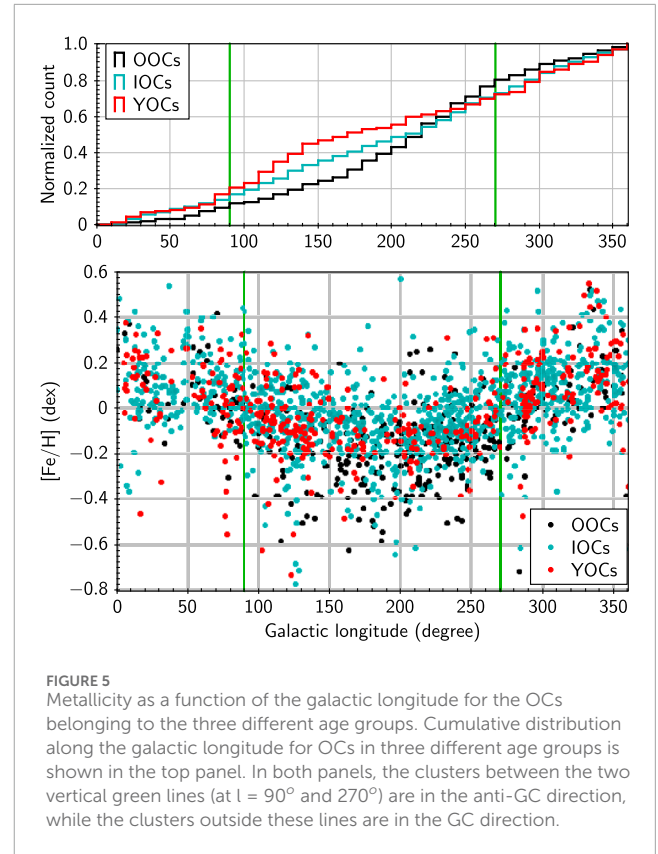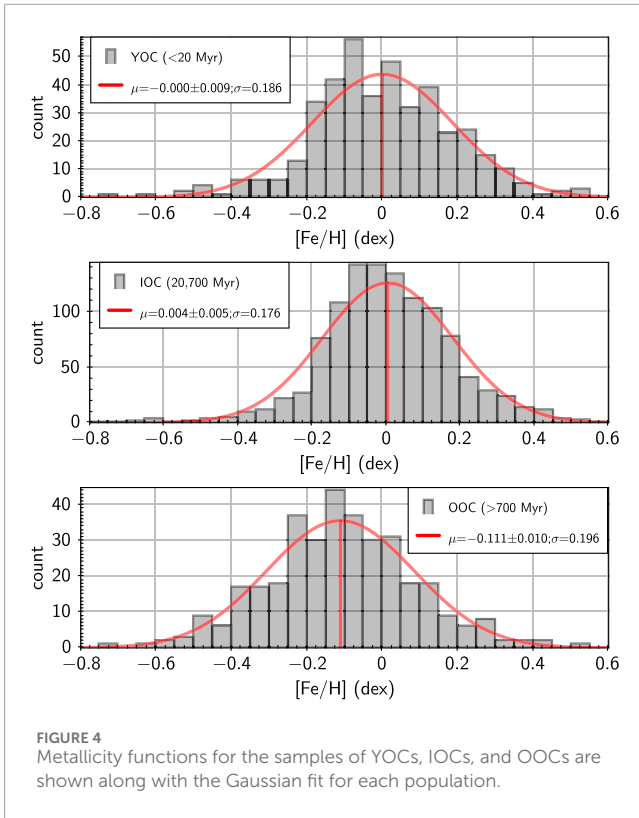
$\frac{d[Fe/H]}{d|Z|}$ (dex kpc^{-1})	$|Z|$ (kpc)	N	Reference
−0.34 ± 0.03	<1.30	63	Piatti et al. (1995)
−0.295 ± 0.050	<1.40	118	Chen et al. (2003)
−0.252 ± 0.039	<0.90	183	Zhong et al. (2020)
−0.545 ± 0.046	<0.487	1814	This work
−0.075 ± 0.093	0.487-1.80	58	This work

Figure 4. For YOC, IOC, and OOC, the mean values of the [Fe/H] distributions are −0.000 ± 0.009, 0.004 ± 0.005, and −0.111 ± 0.010, respectively, and the corresponding sample standard deviations are 0.186, 0.176, and 0.196, respectively. There is hardly any significant difference in metallicity between YOCs and IOCs. However, slightly higher mean metallicity for the YOC and IOC compared to OOC is apparent, which is well-expected as the clusters belonging to YOC and IOC are understood to have formed from gas and dust in the thin disk of the galaxy that has already been enriched through the earlier generation of stellar formation. Additionally, as seen from the figure, the metallicity functions for the OCs of different age groups are not symmetric and are slightly skewed. The skewness values for YOC, IOC, and OOC samples are −0.175, −0.212, and 0.083, respectively. All three age group OC samples span almost similar ranges in metallicity. The metal-poor clusters in the YOC sample have likely formed from the fall of a metal-poor gas to the younger thin disk along with the succeeding starburst. This in-fall of a metal-poor gas is believed to be due to merging satellite galaxies to the Milky Way (Wyse, 1999), resulting in diluting the metallicity of interstellar material in the galactic thin disk and, subsequently, triggering the formation of a large number of metal-poor clusters. On the other hand, the super solar metallicity clusters in the OOC group may have formed from the highly processed material from the inner region of the galaxy. It is believed that the metal-rich old clusters in the inner region had migrated outward the outer disk over a period of time in order to survive the destruction due to relatively stronger galactic potential in the inner disc (Myers et al., 2022a; Magrini, 2023).

To further understand the reason behind the almost-similar large spread in metallicity distribution for OCs of different age groups, we looked into the distribution of [Fe/H] as a function of the galactic longitude. As shown in the bottom panel of Figure 5, clusters toward the anti-GC direction (i.e., with $90^o < l < 270^o$) have relatively lower metallicity than the

cluster in the GC direction (i.e., with $270^o < l < 90^o$). The reason behind this asymmetry is that most of the star-forming regions are in the GC direction where the nucleosynthesis process is more active in comparison to fewer star-forming regions present in the anti-GC direction. As a result, metallicity increases as the stellar evolution progresses. The top panel of the figure shows the cumulative distribution functions (CDFs) for the three age groups and suggests that all three age populations span a similar range in the galactic longitude. We further performed the Kolmogorov–Smirnov (KS) test to check if the three CDFs come from the same distribution. The KS test p-value for the OOC and IOC pair is 0.98, for the IOC and YOC pair is 0.87, and for the OOC and YOC pair is 0.50, hence suggesting that all three CDFs follow the same distribution at a minimum of 50% significance level.

5 Metallicity gradients along the vertical and radial directions

5.1 Vertical metallicity gradient

The metallicity distribution in the Milky Way and its spatial variation is associated with the formation and evolution history of the galaxy. The metallicity distribution at a particular point in the disk is linked with many parameters, like the gas accretion

FIGURE 4
Metallicity functions for the samples of YOCs, IOCs, and OOCs are shown along with the Gaussian fit for each population.

FIGURE 5
Metallicity as a function of the galactic longitude for the OCs belonging to the three different age groups. Cumulative distribution along the galactic longitude for OCs in three different age groups is shown in the top panel. In both panels, the clusters between the two vertical green lines (at l = 90° and 270°) are in the anti-GC direction, while the clusters outside these lines are in the GC direction.

rate, formation history, and evolution at that point of the disk. Previous studies (Marsakov et al., 2005; Marsakov and Borkova, 2006; Soubiran, 2008) indicate that vertical metallicity distribution profiles can provide extremely meaningful ways for separating the thin disk from the thick disk. For our sample of OCs, metallicity as a function of vertical distance (Z) is shown in the left-side panel of Figure 6. The distribution readily suggests a decrease in [Fe/H] as we move away from the galactic plane in both the Northern and Southern hemispheres. To find the metallicity gradient in both the hemispheres, we divide the sample about the center of the galactic mid-plane (i.e., at $Z = 0$). Linear fits to cluster in the Southern (blue-colored points) and Northern hemispheres (red-colored points) are shown as gray and black lines, respectively, and the obtained metallicity gradients are as follows:

$$\frac{d\,[\text{Fe/H}]}{dZ} = 0.380 \pm 0.040 \ \text{dex kpc}^{-1}, \quad -2 < Z < 0 \ kpc, \quad (6)$$
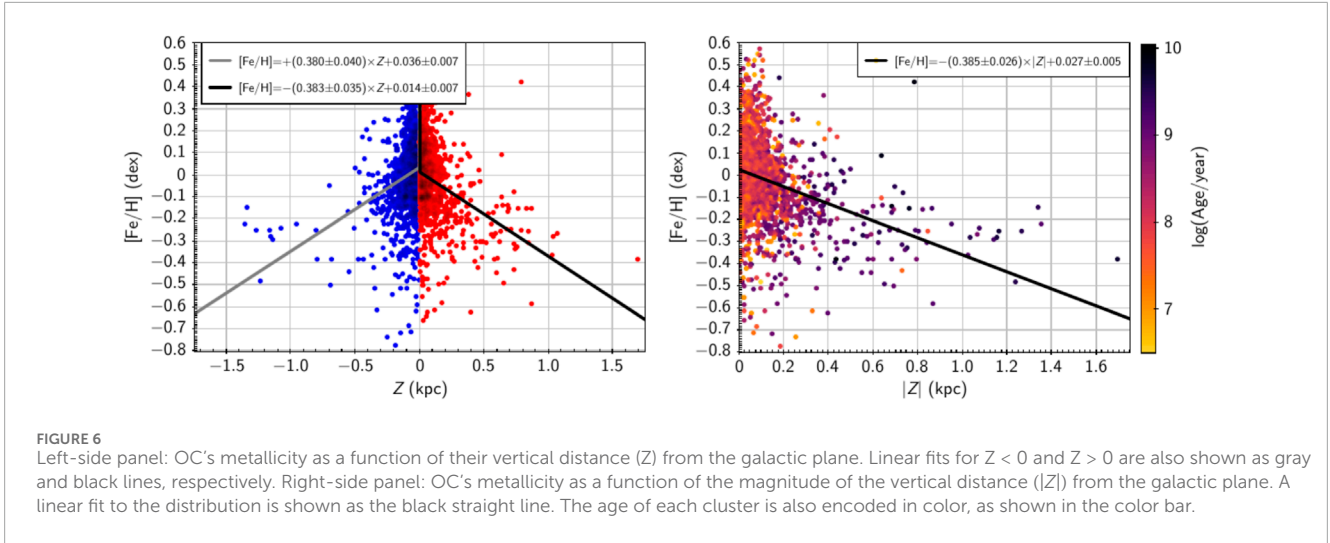
$$\frac{d\,[\text{Fe/H}]}{dZ} = -0.383 \pm 0.035 \ \text{dex kpc}^{-1}, \quad 0 < Z < 2 kpc. \quad (7)$$

The magnitude of the metallicity gradient in both the Northern and Southern hemispheres is nearly the same and indicates that in both hemispheres, metallicity changes at almost similar rates as we move away from the galactic mid-plane. To find the average value of the metallicity gradient, as shown in the right-side panel of Figure 6, we plotted [Fe/H] as a function of the absolute vertical distance from the galactic plane. The metallicity gradient from a linear fit is as follows:

$$\frac{d\,[\text{Fe/H}]}{d|Z|} = -0.385 \pm 0.026 \ \text{dex kpc}^{-1}, \quad |Z| < 2 \ kpc, \quad (8)$$

where the negative slope indicates that metallicity decreases as we move away from the galactic mid-plane. These average vertical-metallicity gradients over a large distance are in agreement with the previous studies. For example, Chen et al. 2003 found a vertical metallicity gradient of -0.295 ± 0.050 dex kpc^{-1} using a sample of 118 OCs. Through a sample of 40,000 stars with low-resolution spectroscopy over 144 lines of sight, Schlesinger et al. (2014) found a vertical metallicity gradient of $-0.243^{+0.039}_{-0.053}$ dex kpc^{-1} in different [α/Fe] subsamples. However, as evident from both panels in Figure 6, a single linear fit is insufficient to explain the full trend in metallicity as a function of the vertical distance. For $|Z| \lesssim 1$ kpc, the metallicity decreases rapidly, while at the larger height, the change is relatively small.

To obtain a more accurate estimate for the vertical metallicity gradient and find the vertical distance at which the radial metallicity gradient changes significantly, we fitted the data with a combination of two linear regressions, and the coefficients of the fitted functions are determined using iterative least square estimation, following the procedure used in Section 3. Based on the distribution in Figure 6, we assumed the initial values of b1, m1, C, and m2 as 1.0, 0.4, 1.0, and 0.0, respectively. The final fitted function is shown as the red line in Figure 7. The coefficients of the fitted functions are also provided in the legends of Figure 7 in the forms b_1, m_1, C, and m_2, where b_1 and m_1 are the y-axis intercept and slope for the first linear function, respectively; m_2 is the slope for the second linear function; and C is the point where these two functions intersect. From the least square fitting, it is found that the two linear functions intersect at

FIGURE 6
Left-side panel: OC's metallicity as a function of their vertical distance (Z) from the galactic plane. Linear fits for Z < 0 and Z > 0 are also shown as gray and black lines, respectively. Right-side panel: OC's metallicity as a function of the magnitude of the vertical distance (|Z|) from the galactic plane. A linear fit to the distribution is shown as the black straight line. The age of each cluster is also encoded in color, as shown in the color bar.

$|Z| = 0.487 \pm 0.087$ kpc, and the vertical metallicity gradients are described as follows:

$$\frac{d\,[\text{Fe/H}]}{d|Z|} = -0.545 \pm 0.046 \ \text{dex kpc}^{-1}, \tag{9}$$
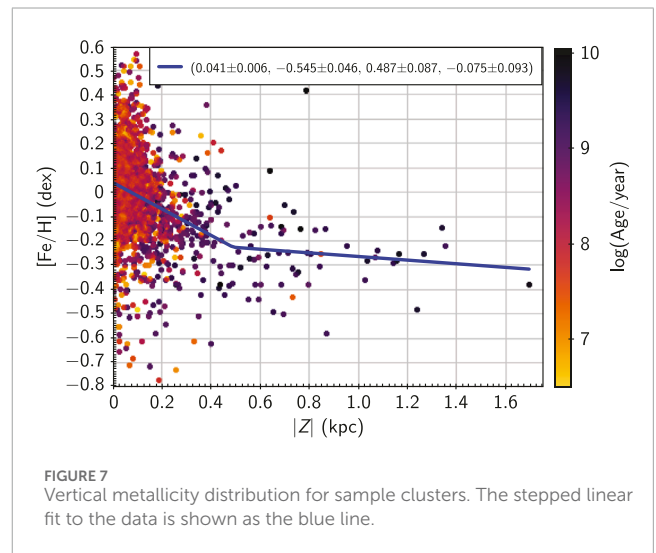
$$0 < |Z| < 0.487 \pm 0.087 \ \text{kpc}$$

$$\frac{d\,[\text{Fe/H}]}{d|Z|} = -0.075 \pm 0.093 \ \text{dex kpc}^{-1}, \tag{10}$$

$$0.487 \pm 0.087 < |Z| \lesssim 1.8 \ \text{kpc}.$$

This stepped vertical-metallicity gradient is in agreement with the currently accepted models of the galaxy having a metal-rich disk (consisting of the thin and thick disk with scale heights of approximately 300 pc and 900 pc, respectively) and a metal-poor stellar halo (e.g., Just et al., 2010; Rix et al., 2013; Matteucci, 2021; and references therein). In Figure 7 (and also in the right-hand panel of Figure 6), cluster ages are also provided in the color of the data point. The figure suggests that the clusters at relatively larger vertical distances are comparatively old apart from being metal-poor. The lower metallicity in these clusters may be explained by their formation in the outer region of the galactic disk at a relatively older time when the interstellar medium was relatively less enriched than the inner region of the galactic disk. In Table 3, we summarize our results along with previous reporting of vertical metallicity gradients.
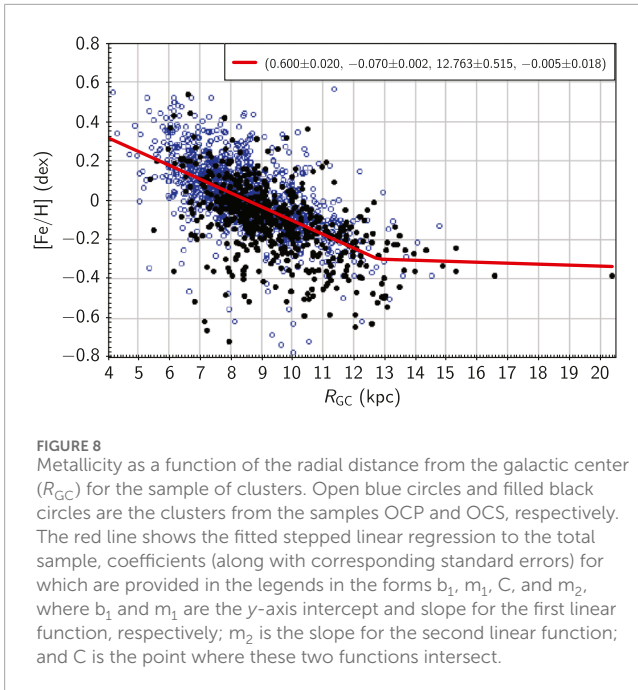
5.2 Radial metallicity gradient

The radial metallicity gradient is another important piece of information to understand the chemical evolution of the galactic disk, and in turn, the evolution of the galaxy as the distribution of metallicity is not homogeneous across the galaxy. It has been found that metallicity in the cluster population shows a decreasing trend with increasing distance from the GC (Wu, 2009; Pancino, 2010; Yong et al., 2012b; Donati et al., 2015b; Magrini et al., 2015; Carrera et al., 2019; Donor, 2020; Zhong et al., 2020; Zhang et al., 2021; Myers et al., 2022a; Netopil, 2022; Spina et al., 2022; Magrini, 2023). The radial metallicity gradient and its evolution with age are among the most critical empirical constraints that one can put on

FIGURE 7
Vertical metallicity distribution for sample clusters. The stepped linear fit to the data is shown as the blue line.

the galactic chemical evolution models. Most of these models show that the formation of clusters strongly influences the appearance and development of radial metallicity gradients (Chiappini et al., 2001), and the precise value of the metallicity gradient in the galactic disk is an important parameter to constrain the chemical evolution models. The existence of such a gradient across the Milky Way disk is well-established through the observations of the HII regions, disk stars, hot stars, star clusters, planetary nebula, Cepheid variables, field stars (Chen et al., 2003; Maciel et al., 2010), and OCs (Carrera et al., 2019; Donor, 2020; Zhong et al., 2020; Zhang et al., 2021; Myers et al., 2022a; Netopil, 2022; Spina et al., 2022; Magrini, 2023). An average gradient of approximately -0.06 dex kpc^{-1} is observed in the Milky Way disk for most of the elements, e.g., O, S, Ne, Ar, and Fe. This magnitude of the observed gradients constrains the various parameters in the chemical evolution model, such as the time scales of star formation and in-fall (Prantzos et al., 1995) or any variations in the stellar initial mass function properties with metallicities (Chiappini et al., 2001).

Star clusters are considered one of the most important celestial sources for investigating the metallicity gradient along the galactic

FIGURE 8
Metallicity as a function of the radial distance from the galactic center (R_{GC}) for the sample of clusters. Open blue circles and filled black circles are the clusters from the samples OCP and OCS, respectively. The red line shows the fitted stepped linear regression to the total sample, coefficients (along with corresponding standard errors) for which are provided in the legends in the forms b_1, m_1, C, and m_2, where b_1 and m_1 are the y-axis intercept and slope for the first linear function, respectively; m_2 is the slope for the second linear function; and C is the point where these two functions intersect.

disk as their distance and age are derived very precisely and are available in a wide range. Metallicity as a function of the radial distance from the GC (R_{GC}) for our sample OC is shown in Figure 8. On average, as expected, the figure suggests a decreasing trend in [Fe/H] with an increase in distance from the GC. Additionally, the figure also suggests that the decrease in [Fe/H] with an increase in R_{GC} is not a simple linear function but at least a combination of two linear functions.

To find radial metallicity gradients and the radial distance at which the radial metallicity gradient changes, we fitted the data with a combination of two linear functions, and the coefficients of the fitted functions are determined using iterative least square estimation adopting the procedure followed in Section 3. Based on the distribution in Figure 8, we assumed the initial values of b1, m1, C, and m2 as 1.0, −0.05, 12.0, and −0.03, respectively. The final fitted function is shown as the red line in the figure. The coefficients of the fitted functions are also provided in the legends of the figure in the forms b_1, m_1, C, and m_2, where b_1 and m_1 are the y-axis intercept and slope for the first linear function, respectively; m_2 is the slope for the second linear function; and C is the point where these two functions intersect. The two linear functions intersect at R_{GC} of 12.763 ± 0.515 kpc, and gradients in R_{GC} metallicity distributions are found as follows:

$$\frac{d\,[\text{Fe/H}]}{dR_{GC}} = -0.070 \pm 0.002 \text{ dex kpc}^{-1},$$

$$4.0 \lesssim R_{GC} \leq 12.763 \pm 0.515 \text{ kpc}, \tag{11}$$

$$\frac{d\,[\text{Fe/H}]}{dR_{GC}} = -0.005 \pm 0.018 \text{ dex kpc}^{-1},$$

$$12.763 \pm 0.515 < R_{GC} \lesssim 20.5 \text{ kpc}. \tag{12}$$

The existence of the two-step linear distribution can be explained in most evolution models by assuming different in-fall and star formation rates for the inner and outer disks. A similar two-step

distribution was also noticed by Lépine (2011), Gozha et al. (2012), Myers et al. (2022a), Magrini (2023), and others. All these studies have found a discontinuity in the radial metallicity gradient at $R_{GC} \sim 10$–12 kpc, with a steeper gradient in the inner disk region and a flatter gradient or a plateau in the outer disk region. However, some other studies have not seen such a two-step distribution, although they found a decreasing trend in metallicity with increasing R_{GC}, e.g., Friel et al., 2002; Chen et al., 2003; Magrini, 2009; and Gaia Collaboration et al., 2023.

Our estimated radial metallicity gradients are in close agreement with some of the recent determinations of metallicity gradients derived using samples of OCs. A comparison of radial metallicity gradients from some of the recent studies based on OCs along with our estimates is provided in Table 4. Most of these studies suggest a radial metallicity gradient of approximately −0.06 dex kpc^{-1}. The radial metallicity gradient provides vital information on radial migration, which plays an important role in the redistribution of stellar populations, particularly the older populations, in our galaxy. It is believed that radial migration in OCs may be the reason for the flattening of the radial metallicity gradient over a period of time (Zhang et al., 2021; Viscasillas Vázquez, 2022). It is believed that there is a deficiency of low-metallicity clusters in the inner disk migrating from the outer disk as the chance of survival in the high galactic potential of the inner disk is low. On the other hand, clusters from the more metal-rich inner galactic disk can migrate farther into the outer disk where the potentials of the spiral arm and bar are weaker, resulting in the enhancement of the mean metallicity of the outer disk. As a consequence, the radial metallicity gradient is steeper in the inner disk while flattening out toward the large galactocentric distance. Various earlier studies using different tracers such as planetary nebulae, classical Cepheids, and globular clusters also suggested that the radial metallicity gradient becomes slightly flatter with time (e.g., Friel et al., 2002; Chen et al., 2003; Maciel et al., 2009; Luck et al., 2011; Genovali et al., 2014; da Silva et al., 2023). It was contemplated by Toyouchi and Masashi (2014) that the radial metallicity gradient was positive at the time of formation of the thick disk, which subsequently became negative during the transition phase of disk formation from the thick to thin disk. It became flatter by the time of the formation of the thin disk. They credited this evolution of the disk to the gas in-fall history having a shorter time scale in the inner disk and a relatively longer time scale in the outer disk, which is often called the 'inside-out' scenario in disk formation.

5.3 Age dependence of radial and vertical metallicity gradients

One of the crucial questions in the chemical evolution of the galaxy is how the metallicity gradients have evolved over the last few Gyrs. As the overall metallicity gradient may introduce a bias due to the mix of different aged OCs, we may need to restrict the sample to OCs in different age bins in order to understand the evolution in the metallicity gradients along the radial and vertical directions with time. The age dependence of the metallicity gradient has been investigated in the past using a variety of sources (e.g., Vickers et al., 2021, and references therein). We, therefore, split our sample broadly into three age bins, including the very young-age bin (< 20 Myr), the young-to-intermediate-age bin (20 Myr–700 Myr), and the old-age bin (> 700 Myr). Since we have less than

TABLE 4 Comparison of radial metallicity gradient $\left(\frac{d[\text{Fe/H}]}{dR_{\text{GC}}}\right)$ among different studies based on the sample of open clusters. The number of clusters (N) used in each of the studies is provided in the third column.

$\frac{d[\text{Fe/H}]}{dR_{\text{GC}}}$	RGC	N	Reference
(dex kpc^{-1})	(kpc)		
-0.059 ± 0.010	7-16	39	Friel et al. (2002)
-0.063 ± 0.008	<17	118	Chen et al. (2003)
-0.056 ± 0.007	<17	488	Wu (2009)
-0.051 ± 0.003	5-15	127	Genovali et al. (2014)
-0.061 ± 0.004	7-13	19	Donor (2018)
-0.052 ± 0.003	6-13	46	Carrera et al. (2019)
-0.077 ± 0.007	6-14.5	90	Carrera et al. (2019)
-0.068 ± 0.001	6-13.9	71	Donor (2020)
-0.053 ± 0.004	7-15	295	Zhong et al. (2020)
-0.074 ± 0.007	6-20	225	Zhang et al. (2021)
-0.066 ± 0.006	6-15.5	157	Zhang et al. (2021)
-0.076 ± 0.009	6-16.5	134	Spina (2021)
-0.073 ± 0.002	6-11.5	94	Myers et al. (2022a)
-0.032 ± 0.002	11.5-16.0	56	Myers et al. (2022a)
-0.054 ± 0.008	5-12	503	Gaia Collaboration et al. (2023)
-0.064 ± 0.007	5-24	175	Spina et al. (2022)
-0.058	6-21	136	Netopil (2022)
-0.054 ± 0.004	6-21	62	Magrini (2023)
-0.081 ± 0.008	6-11.2	42	Magrini (2023)
-0.044 ± 0.014	11.2-21	20	Magrini (2023)
-0.070 ± 0.002	4.0-12.8	1837	This work
-0.005 ± 0.018	12.8-20.5	35	This work

TABLE 5 Radial and vertical metallicity gradients for OCs of different age groups. The number of clusters (N) in each of the age bin is provided in the fourth column.

Age	$\frac{d[\text{Fe/H}]}{dR_{\text{GC}}}$	$\frac{d[\text{Fe/H}]}{dZ}$	N
(Myr)	(dex kpc^{-1})	(dex kpc^{-1})	
<20	-0.063 ± 0.005	-0.427 ± 0.148	410
20–700	-0.071 ± 0.003	-0.459 ± 0.061	1,114
>700	-0.058 ± 0.004	-0.245 ± 0.032	349

For the three age distributions, we also examined the vertical metallicity gradient, i.e., the change in the metallicity as a function of galactic disk thickness. We found a steeper slope for the young and intermediate-age OCs, while it is shallower for the old OCs. The estimated slope values are given in the third column of Table 5. This behavior of OCs is well-expected because most of the young and intermediate-age OCs lie closer to the metal-rich thin galactic disk, while older OCs are located farther away in the metal-poor outer disk. Carrera et al. (2019), however, do not find any evidence of the presence of a vertical metallicity gradient, at least above the 1-σ level. A further examination of the vertical evolution of the metallicity gradient is performed in the next section.

5.4 Vertical evolution of the radial metallicity gradient

The study of the relation between the metallicity and the location of the cluster on the galactic disk is an important tool for the study of the structure formation and evolution of the galaxy (e.g., Zhong et al., 2020). We also investigated the evolution of radial metallicity gradients in the vertical direction of the galactic plane as clusters are widely distributed in the vertical direction of the galactic disk. The effect of the scale height on the rate of change in metallicity variation with the R_{GC} has been analyzed by plotting the slope of the radial metallicity gradients as a function of the absolute value of Z, which is shown in Figure 9. $|Z|$ for our sample ranges from 0 to approximately 1.8 kpc (excluding one lone cluster located at approximately 2.6 kpc). Although most of the clusters are located near the galactic plane, there are fewer clusters at larger vertical distances. Therefore, we considered a varying bin size in the Z scale. We considered a bin width of 50 pc for $|Z| < 200$, 100 pc for $200 < |Z| < 400$, and 500 pc for $|Z| > 400$ by making sure that there are enough clusters in the selected bins to get a proper estimate of the radial metallicity gradient. As shown in Figure 9, the variation in $\frac{d[\text{Fe/H}]}{dR_{\text{GC}}}$ as a function of the absolute vertical distance $|Z|$ for our sample of OCs follows an increasing trend with an increase in $|Z|$. The estimated standard errors in $\frac{d[\text{Fe/H}]}{dR_{\text{GC}}}$ and mean $|Z|$ are shown as black colored cross bars. At larger vertical distances, the estimated errors are larger because of the smaller sample size in the corresponding vertical distance bins. A linear fit to the distribution is shown as a thick red line, and the corresponding coefficients are shown in the legends. The radial metallicity gradient $\left(\frac{d[\text{Fe/H}]}{dR_{\text{GC}}}\right)$, as a function of the vertical distance from the galactic plan, is found to vary at a rate of 0.068 ± 0.016 dex kpc^{-1} kpc^{-1}, suggesting a higher

10% of the OCs older than 1 Gyr, we have not split the bins in the older age regime. Table 5 shows the slopes for the graphs in various age bins. Along the radial direction, the three age populations have almost similar metallicity gradients, except for the youngest clusters, which have a slightly shallower gradient than the intermediate-age clusters. The lower (or flatter) gradient in the case of the older population is in agreement with previous studies and models and could be explained by the chemical evolution in the galactic disk (Chang et al., 2002; Jacobson et al., 2016; Zhong et al., 2020) and radial migration (Netopil, 2016; Anders, 2017). For example, in the MCM model, radial migration is expected to flatten the radial metallicity gradient for clusters older than one Gyr (Minchev et al., 2014).
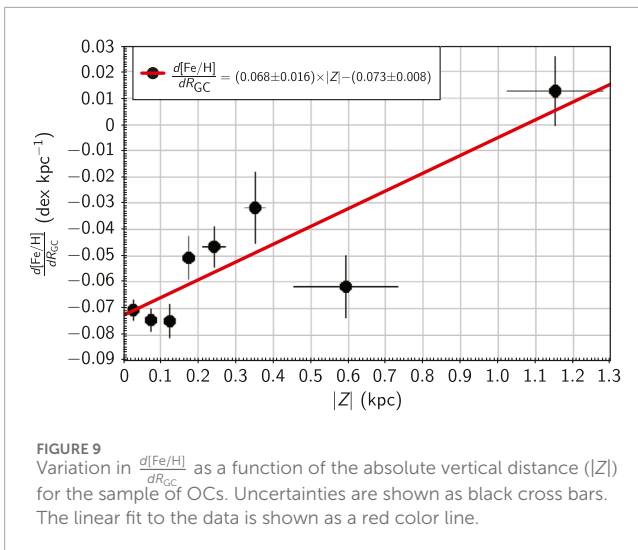
FIGURE 9
Variation in $\frac{d[Fe/H]}{dR_{GC}}$ as a function of the absolute vertical distance ($|Z|$) for the sample of OCs. Uncertainties are shown as black cross bars. The linear fit to the data is shown as a red color line.

rate of change of metallicity with R_{GC} at a larger vertical distance from the galactic plane. The radial metallicity gradient at the center of the galactic plane is estimated as -0.073 ± 0.008 dex kpc^{-1}, which is in agreement with our previous estimate shown in Section 4.2.

6 Discussion and conclusion

In this study, we used the largest sample of 1,879 open clusters to understand the distribution and evolution of metallicity in the galactic disk. The cluster sample was compiled from the literature with available metallicity information along with other information like age, position coordinates, distances, and radial and vertical distances. About 90% of the OCs in our sample are younger than 1 Gyr, with the oldest being about 10 Gyr old. Radially and vertically, about 90% of the clusters in our sample are within a heliocentric distance of 3 kpc, while about 97% of the clusters are within a vertical distance of 500 pc, practically restricting our study to the galactic disk.

The age–metallicity relation provides an important constraint on the theoretical models of the disk and, thus, has been studied multiple times in the past. The study of metallicity evolution for our sample of OCs did not find a strict age–metallicity relation, but a stepped linear evolution of metallicity in the galaxy was observed with a discontinuity at log(age/year) = 8.378 ± 0.093 at the age of approximately 240 Myr. OCs older than 240 Myr follow a decreasing trend in metallicity with an increase in age, with an age–metallicity gradient of -0.031 ± 0.006 dex/Gyr, which is in agreement with some of the recent studies as well as the galactic evolutionary models. The slightly higher average metallicity in the intermediate age clusters compared to the average metallicity in the young ones agrees with findings in earlier studies (Pancino, 2010; Zhong et al., 2020). Interestingly, the sample of OCs younger than about 240 Myr follows a slightly increasing trend in metallicity with an increase in age. The radial and vertical migration of young OCs in the disk is suspected to be one of the main reasons for this weak correlation between log(age) and [Fe/H] for younger clusters. However, no strong correlation has been found to draw any meaningful conclusion. Despite a large scatter in the age–metallicity relation in our study, it is crucial to observe the slightly different

age–metallicity relation for two different samples of clusters, which possibly applied distinct formation constraints on the galactic thin and thick disc in modeling the Milky Way.

It is well-understood that the metallicity in the inner region of the galactic disk is increasing with time (e.g., Reddy, 2003; Haywood et al., 2013, and references therein). Hence, the younger clusters with lower metallicity must have either formed away from the galactic plane or in the anti-GC direction. To see whether the latter is the reason behind lower metallicity in younger clusters, we investigated the distribution of metallicity in the galactic plane by plotting metallicity as a function of the galactic longitude. The OCs in the anti-GC direction do have lower metallicity compared to the OCs in the GC direction, possibly owing to the differences in timelines of gas in-falls and formation of clusters in the GC and anti-GC directions. Our samples of YOCs, IOCs, and OOCs are found to equally populate both the GC and anti-GC directions, hence leaving vertical migration as one of the likely reasons for slightly lower metallicity in younger clusters.

Using our sample of clusters, we further explored the vertical and radial metallicity gradients in the galactic disk. Metallicity was found to follow a stepped variation with vertical distance from the galactic plane. Near the galactic plane, with $|Z| < 0.487 \pm 0.087$ kpc, we estimated the vertical metallicity gradient of -0.545 ± 0.046 dex kpc^{-1}, while for a large vertical distance having $0.487 \pm 0.087 < |Z| \lesssim 1.8$ kpc, we found a lower vertical metallicity gradient of -0.075 ± 0.093 dex kpc^{-1}. The lower metallicity gradient at large vertical distances compared to the one at smaller vertical distances agrees with the galactic chemical evolution models. We found that most of the OCs at large vertical distances are older compared to the majority of the clusters located near the galactic plane. This difference in the ages of clusters from the two vertical regions is believed to be the main reason for the flatter vertical metallicity gradient at large vertical distances compared to the steep vertical metallicity gradient at smaller vertical distances.

Similar to the vertical direction, the change in metallicity in the radial direction is also found to follow a stepped linear relation. For a radial distance between approximately 4.0 and 12.8 kpc, we found a radial metallicity gradient $\left(\frac{d[Fe/H]}{dR_{GC}}\right)$ of -0.070 ± 0.002 dex kpc^{-1}, while for a radial distance between approximately 12.8 and 20.5 kpc, we found a much smaller radial metallicity gradient of -0.005 ± 0.018 dex kpc^{-1}. Thus, the OCs in the outer galactic disc are generally more metal-poor than the OCs in the inner galactic disc and in the solar neighborhood. Although a shallower metallicity gradient in the region 12.8–20.5 kpc may be biased due to the relatively smaller number of OCs at larger galactocentric distances, it could also be the result of radial migration of clusters in the galactic disk (Zhang et al., 2021). Using a smaller sample of 295 OCs within a galactocentric distance of 7–15 kpc, Zhong et al. (2020) reported a steeper slope of -0.252 ± 0.039 dex kpc^{-1}. It should also be noted that a significant variation in the slope and the turn-off point in the radial metallicity gradient among different studies comes from the choice of the cluster sample, selected range of R_{GC}, and unequal vertical heights. Overall, our radial metallicity gradient estimates agree with most of the recent studies (Reddy et al. 2020; Zhang et al. 2021; Myers et al. 2022a).

One of the key questions in the galactic chemical evolution models is the evolution of the radial metallicity gradients over time,

and the answer is not determined yet. We, therefore, examined the time evolution of the metallicity gradients, both in radial and vertical directions, with age, by dividing the clusters into three age bins of < 20 Myr, 20–700 Myr, and > 700 Myr. We observed that these gradients are shallower for the oldest age bin, while not much difference was noticeable in the young and intermediate-age clusters. The time evolution of abundance gradients has also been examined in the past, but an unequivocal result has not been found so far. Although Vincenzo et al. (2018) and Minchev et al. (2018) suggested a flatter metallicity gradient with time, there are a few studies like Chiappini et al. (2001) and Mott et al. (2013), which suggested a steepening in gradient over time. However, the variation is only prominent over a longer time scale, and the limited temporal coverage of the present cluster sample, where only a small number of OCs are available beyond the 1 Gyr period, in no way sheds any more light on this discussion. We refer Magrini (2023) for a more detailed discussion on the temporal evolution of the metallicity gradients.

We further studied the variation in the radial metallicity gradient with distance from the galactic plane and found that the radial metallicity gradient linearly increases with an increase in the vertical distance and obtained a radial metallicity gradient slope of $\frac{d[\text{Fe/H}]}{dR_{\text{GC}}} = 0.068 \pm 0.016$ dex kpc^{-1} kpc^{-1} as a function of vertical distance from the galactic plane. This agrees with the galactic evolutionary models, for example, see Toyouchi and Masashi (2014) and references therein. In the case of a thin disk, which has a scale height of approximately 300 pc, the radial metallicity gradient is highly negative even though it linearly increases with the vertical distance from the galactic plane. However, for the thick disk (having a typical scale height of approximately 900 pc), the radial metallicity gradient is slightly high and approaches zero at approximately 1 kpc. Toyouchi and Masashi (2014) suggested that the radial metallicity gradient was positive at the time of formation of the thick disk but subsequently became negative during the transition phase of the disk formation from the thick to thin disk. The gradient became flatter by the time of the formation of the thin disk. This change in the radial metallicity gradient with a vertical distance is believed to be related to the gas in-fall history in the galaxy. A large negative radial metallicity gradient near the galactic plane (i.e., in the thin disk) but a higher gradient in the case of the thick disk (i.e., large vertical distance) can be explained by the shorter and longer time scales, respectively, for the gas in-fall.

Data availability statement

The original contributions presented in the study are included in the article/supplementary material; further inquiries can be directed to the corresponding author.

References

Allen, C., Carigi, L., and Peimbert, M. (1998). Chemodynamical model of the Galaxy: abundance gradients predicted for H II regions and planetary nebulae. *Astrophysical J.* 494 (1), 247–255. doi:10.1086/305204

Anders, F., Chiappini, C., Minchev, I., Miglio, A., Montalbán, J., Mosser, B., et al. (2017). Red giants observed by CoRoT and APOGEE: the evolution of the Milky

Author contributions

YJ: writing–original draft, conceptualization, methodology, and resources. D: formal analysis, writing–review and editing, data curation, methodology, investigation, and validation. SM: data curation and writing–review and editing.

Conflict of interest

The authors declare that the research was conducted in the absence of any commercial or financial relationships that could be construed as a potential conflict of interest.

Publisher's note

All claims expressed in this article are solely those of the authors and do not necessarily represent those of their affiliated organizations, or those of the publisher, the editors, and the reviewers. Any product that may be evaluated in this article, or claim that may be made by its manufacturer, is not guaranteed or endorsed by the publisher.

Supplementary material

The Supplementary Material for this article can be found online at: https://www.frontiersin.org/articles/10.3389/fspas.2024.1348321/full#supplementary-material

Way's radial metallicity gradient. *Astronomy Astrophysics* 600, A70. [astro-ph.GA]. doi:10.1051/0004-6361/201629363

Andrievsky, S. M., Kovtyukh, V. V., Luck, R. E., Lépine, J. R. D., Bersier, D., Maciel, W. J., et al. (2002). Using Cepheids to determine the galactic abundance gradient. I. The solar neighbourhood. *Astronomy Astrophysics* 381, 32–50. [astro-ph]. doi:10.1051/0004-6361/20011488

Baratella, M., D'Orazi, V., Carraro, G., Desidera, S., Randich, S., Magrini, L., et al. (2020). The Gaia-ESO Survey: a new approach to chemically characterising young open clusters. I. Stellar parameters, and iron-peak, α-and proton-capture elements. *Astronomy Astrophysics* 634, A34. [astro-ph.SR]. doi:10.1051/0004-6361/201937055

Bobylev, V. V., and Bajkova, A. T. (2019). Kinematics of the Galaxy from a sample of young open star clusters with data from the Gaia DR2 catalogue. *Astron. Lett.* 45 (3), 109–119. [astro-ph.GA]. doi:10.1134/s1063773719030010

Bragaglia, A., Sestito, P., Villanova, S., Carretta, E., Randich, S., and Tosi, M. (2008). Old open clusters as key tracers of Galactic chemical evolution: II. Iron and elemental abundances in NGC 2324, NGC 2477, NGC 2660, NGC 3960, and Berkeley 32. *Astronomy Astrophysics* 480 (1), 79–90. doi:10.1051/0004-6361:20077904

Caetano, T. C., Dias, W., Lépine, J., Monteiro, H., Moitinho, A., Hickel, G., et al. (2015). The OPD photometric survey of open clusters I. Techniques, program details and first results of robust determination of the fundamental parameters. *New Astron.* 38, 31–49. doi:10.1016/j.newast.2015.01.003

Cantat-Gaudin, T., Anders, F., Castro-Ginard, A., Jordi, C., Romero-Gómez, M., Soubiran, C., et al. (2020). Painting a portrait of the Galactic disc with its stellar clusters. *Astronomy Astrophysics* 640, A1. [astro-ph.GA]. doi:10.1051/0004-6361/202038192

Cantat-Gaudin, T., Jordi, C., Vallenari, A., Bragaglia, A., Balaguer-Núñez, L., Soubiran, C., et al. (2018). A Gaia DR2 view of the open cluster population in the Milky Way. *Astronomy Astrophysics* 618, A93. [astro-ph.GA]. doi:10.1051/0004-6361/201833476

Carraro, G., Bresolin, F., Villanova, S., Matteucci, F., Patat, F., and Romaniello, M. (2004). Metal abundances in extremely distant galactic old open clusters. I. Berkeley 29 and saurer 1. *Astronomical J.* 128 (4), 1676–1683. [astro-ph]. doi:10.1086/423912

Carraro, G., Geisler, D., Villanova, S., Frinchaboy, P. M., and Majewski, S. R. (2007a). Old open clusters in the outer Galactic disk. *Astronomy Astrophysics* 476 (1), 217–227. [astro-ph]. doi:10.1051/0004-6361:20078113

Carraro, G., Moitinho, A., Zoccali, M., Vázquez, R. A., and Baume, G. (2007b). Photometry of a galactic field at $l = 232°, b = -6°$: the old open cluster auner 1, the norma-Cygnus spiral arm, and the signature of the warped galactic thick disk. *Astronomical J.* 133 (3), 1058–1066. [astro-ph]. doi:10.1086/510331

Carraro, G., Ng, Y. K., and Laura, P. (1998). On the Galactic disc age-metallicity relation. *Mon. Notices RAS* 296 (4), 1045–1056. [astro-ph]. doi:10.1046/j.1365-8711.1998.01460.x

Carraro, G., Villanova, S., Demarque, P., Bidin, C. M., and McSwain, M. V. (2008). The old open cluster NGC 2112: updated estimates of fundamental parameters based on a membership analysis. *Mon. Notices RAS* 386 (3), 1625–1634. [astro-ph]. doi:10.1111/j.1365-2966.2008.13143.x

Carrera, R. (2012). Radial velocities and metallicities from infrared Ca II triplet spectroscopy of open clusters: Berkeley 26, Berkeley 70, NGC 1798, and NGC 2266★. *Astronomy Astrophysics* 544, A109. [astro-ph.GA]. doi:10.1051/0004-6361/201219625

Carrera, R., Bragaglia, A., Cantat-Gaudin, T., Vallenari, A., Balaguer-Núñez, L., Bossini, D., et al. (2019). Open clusters in APOGEE and GALAH. Combining Gaia and ground-based spectroscopic surveys. *Astronomy Astrophysics* 623, A80. [astro-ph.GA]. doi:10.1051/0004-6361/201834546

Carrera, R., Casamiquela, L., Ospina, N., Balaguer-Núñez, L., Jordi, C., and Monteagudo, L. (2015). Radial velocities and metallicities from infrared Ca ii triplet spectroscopy of open clusters: II. Berkeley 23, King 1, NGC 559, NGC 6603, and NGC 7245★★★. *Astronomy Astrophysics* 578, A27. [astro-ph.SR]. doi:10.1051/0004-6361/201425531

Carrera, R., and Pancino, E. (2011). Chemical abundance analysis of the open clusters Berkeley 32, NGC 752, Hyades, and Praesepe. *Astronomy Astrophysics* 535, A30. [astro-ph.GA]. doi:10.1051/0004-6361/201117473

Casamiquela, L., Blanco-Cuaresma, S., Carrera, R., Balaguer-Núñez, L., Jordi, C., Anders, F., et al. (2019). OCCASO - III. Iron peak and α elements of 18 open clusters. Comparison with chemical evolution models and field stars. *Mon. Notices RAS* 490 (2), 1821–1842. [astro-ph.GA]. doi:10.1093/mnras/stz2595

Casamiquela, L., Soubiran, C., Jofré, P., Chiappini, C., Lagarde, N., Tarricq, Y., et al. (2021). Abundance-age relations with red clump stars in open clusters. *Astronomy Astrophysics* 652, A25. [astro-ph.GA]. doi:10.1051/0004-6361/202039951

Chang, R.-X., Shu, C.-G., and Jin-Liang, H. (2002). History of star formation and chemical enrichment in the Milky way disk. *Chin. J. Astronomy Astrophysics* 2, 226–247. doi:10.1088/1009-9271/2/3/226

Chen, L., et al. (2008). "Open clusters: their kinematics and metallicities". In: *A giant step: from milli-to micro-arcsecond astrometry*, IAU Symposium, 433–439. doi:10.1017/S1743921308019765

Chen, L., Hou, J. L., and Wang, J. J. (2003). On the galactic disk metallicity distribution from open clusters. I. New catalogs and abundance gradient. *Astronomical J.* 125 (3), 1397–1406. [astro-ph]. doi:10.1086/367911

Chiappini, C., Matteucci, F., and Donatella, R. (2001). Abundance gradients and the formation of the Milky way. *Astrophysical J.* 554 (2), 1044–1058. [astro-ph]. doi:10.1086/321427

Claria, J. J., Lapasset, E., and Minniti, D. (1989). Photometric metal abundances of high-luminosity red stars,in young and intermediate-age open clusters. *Astronomy Astrophysics* 78, 363–374.

Clariá, J. J., Piatti, A., Mermilliod, J., and Palma, T. (2008). Photometric membership and metallicities of red giant candidates in selected open clusters. *Astron. Nachrichten* 329 (6), 609–618. doi:10.1002/asna.200710970

Clariá, J. J., Piatti, A. E., Lapasset, E., and Mermilliod, J. C. (2003). Multicolour photometry and Coravel observations of stars in the southern open cluster IC 2488. *Astronomy Astrophysics* 399, 543–551. doi:10.1051/0004-6361:20021828

Conrad, C., Scholz, R. D., Kharchenko, N. V., Piskunov, A. E., Schilbach, E., Röser, S., et al. (2014). A RAVE investigation on Galactic open clusters: I. Radial velocities and metallicities★. *Astronomy Astrophysics* 562, A54. [astro-ph.SR]. doi:10.1051/0004-6361/201322070

Daflon, S., and Cunha, K. (2004). Galactic metallicity gradients derived from a sample of OB stars. *Astrophysical J.* 617 (2), 1115–1126. [astro-ph]. doi:10.1086/425607

da Silva, R., D'Orazi, V., Palla, M., Bono, G., Braga, V. F., Fabrizio, M., et al. (2023). Oxygen, sulfur, and iron radial abundance gradients of classical Cepheids across the Galactic thin disk. *Astronomy Astrophysics* 678, A195. [astro-ph.GA]. doi:10.1051/0004-6361/202346982

De Silva, G. M., Carraro, G., D'Orazi, V., Efremova, V., Macpherson, H., Martell, S., et al. (2015). Binary open clusters in the Milky Way: photometric and spectroscopic analysis of NGC 5617 and Trumpler 22. *Mon. Notices RAS* 453 (1), 106–112. [astro-ph.SR]. doi:10.1093/mnras/stv1583

De Silva, G. M., Freeman, K. C., Asplund, M., Bland-Hawthorn, J., Bessell, M. S., and Collet, R. (2007). Chemical homogeneity in collinder 261 and implications for chemical tagging. *Astronomical J.* 133 (3), 1161–1175. [astro-ph]. doi:10.1086/511182

Dias, W. S., Monteiro, H., Moitinho, A., Lépine, J. R. D., Carraro, G., Paunzen, E., et al. (2021). Updated parameters of 1743 open clusters based on Gaia DR2. *Mon. Notices RAS* 504 (1), 356–371. [astro-ph.SR]. doi:10.1093/mnras/stab770

Donati, P., Cocozza, G., Bragaglia, A., Pancino, E., Cantat-Gaudin, T., Carrera, R., et al. (2015a). The old, metal-poor, anticentre open cluster Trumpler 5. *Mon. Notices RAS* 446 (2), 1411–1423. [astro-ph.SR]. doi:10.1093/mnras/stu2162

Donati, P., Cocozza, G., Bragaglia, A., Pancino, E., Cantat-Gaudin, T., Carrera, R., et al. (2015b). The old, metal-poor, anticentre open cluster Trumpler 5. *Mon. Notices RAS* 446 (2), 1411–1423. [astro-ph.SR]. doi:10.1093/mnras/stu2162

Döner, S., Ak, S., Önal Taş, Ö., and Plevne, O. (2023). The age-metallicity relation in the solar neighbourhood. *Phys. Astronomy Rep.* 1 (1), 11–26. [astro-ph.GA]. doi:10.26650/par.2023.00002

Donor, J., Frinchaboy, P. M., Cunha, K., O'Connell, J. E., Prieto, C. A., Almeida, A., et al. (2020). The open cluster chemical abundances and mapping survey. IV. Abundances for 128 open clusters using SDSS/APOGEE DR16. *Astronomical J.* 159 (5), 199. [astro-ph.GA]. doi:10.3847/1538-3881/ab77bc

Donor, J., Frinchaboy, P. M., Cunha, K., Thompson, B., O'Connell, J., Zasowski, G., et al. (2018). The open cluster chemical abundances and mapping survey. II. Precision cluster abundances for APOGEE using SDSS DR14. *Astronomical J.* 156 (4), 142. [astro-ph.GA]. doi:10.3847/1538-3881/aad635

D'Orazi, V., and Randich, S. (2009). Chemical composition of the young open clusters IC 2602 and IC 2391. *Astronomy Astrophysics* 501 (2), 553–562. [astro-ph.SR]. doi:10.1051/0004-6361/200811587

Edvardsson, B., et al. (1993). The chemical evolution of the galactic disk. I. Analysis and results. *Astronomy Astrophysics* 500, 391–442.

Feltzing, S., Holmberg, J., and Hurley, J. R. (2001). The solar neighbourhood age-metallicity relation - does it exist? *Astronomy Astrophysics* 377, 911–924. [astro-ph]. doi:10.1051/0004-6361:20011119

Ford, A., Jeffries, R. D., and Smalley, B. (2005). Elemental abundances in the Blanco 1 open cluster. *Mon. Notices RAS* 364 (1), 272–282. [astro-ph]. doi:10.1111/j.1365-2966.2005.09562.x

Fossati, L., Folsom, C. P., Bagnulo, S., Grunhut, J. H., Kochukhov, O., Landstreet, J. D., et al. (2011). A detailed spectroscopic analysis of the open cluster NGC 5460. *Mon. Notices RAS* 413 (2), 1132–1144. [astro-ph.SR]. doi:10.1111/j.1365-2966.2011.18199.x

Friel, E. D. (1995). The old open clusters of the Milky way. *Annu. Rev. Astron Astrophysis* 33, 381–414. doi:10.1146/annurev.aa.33.090195.002121

Friel, E. D. (2013). "Open clusters and their role in the Galaxy". In: *Planets, stars and stellar systems*. Ed. by D. O. Terry, and G. Gerard, Springer, Berlin, Germany. doi:10.1007/978-94-007-5612-0_7

Friel, E. D., and Boesgaard, A. M. (1992). Chemical composition of open clusters. III. Iron and carbon in F dwarfs in coma, praesepe, and M67. *Astrophysical J.* 387, 170. doi:10.1086/171069

Friel, E. D., Jacobson, H. R., and Pilachowski, C. A. (2010). Abundances of red giants in old open clusters. V. Be 31, Be 32, Be 39, M 67, NGC 188, and NGC 1193. *Astronomical J.* 139 (5), 1942–1967. doi:10.1088/0004-6256/139/5/1942

Friel, E. D., Janes, K. A., Tavarez, M., Scott, J., Katsanis, R., Lotz, J., et al. (2002). Metallicities of old open clusters. *Astronomical J.* 124 (5), 2693–2720. doi:10.1086/344161

Frinchaboy, P. M., et al. (2004). Star clusters in the galactic anticenter stellar structure: new radial velocities and metallicities. https://arxiv.org/abs/astro-ph/0411127.

Frinchaboy, P. M., Thompson, B., Jackson, K. M., O'Connell, J., Meyer, B., Zasowski, G., et al. (2013a). The open cluster chemical analysis and mapping survey: local galactic metallicity gradient with APOGEE using SDSS DR10. *Astrophysical J. Lett.* 777 (1), L1. [astro-ph.GA]. doi:10.1088/2041-8205/777/1/l1

Frinchaboy, P. M., Thompson, B., Jackson, K. M., O'Connell, J., Meyer, B., Zasowski, G., et al. (2013b). The open cluster chemical analysis and mapping survey: local galactic metallicity gradient with APOGEE using SDSS DR10. *Astrophysical J. Lett.* 777 (1), L1. [astro-ph.GA]. doi:10.1088/2041-8205/777/1/l1

Fu, X., Bragaglia, A., Liu, C., Zhang, H., Xu, Y., Wang, K., et al. (2022). LAMOST meets Gaia: the Galactic open clusters. *Astronomy Astrophysics* 668, A4. [astro-ph.GA]. doi:10.1051/0004-6361/202243590

Gaia Collaboration (2016). The Gaia mission. *Astronomy Astrophysics* 595, A1. [astro-ph.IM]. doi:10.1051/0004-6361/201629272

Gaia Collaboration (2023). Gaia data release 3. Chemical cartography of the Milky way. *Astronomy Astrophysics* 674, A38. [astro-ph.GA]. doi:10.1051/0004-6361/202243511

Geisler, D., Villanova, S., Carraro, G., Pilachowski, C., Cummings, J., Johnson, C. I., et al. (2012). The unique Na:O abundance distribution in NGC 6791: the first open(?) cluster with multiple populations. *Astrophysical J. Lett.* 756 (2), L40. [astro-ph.GA]. doi:10.1088/2041-8205/756/2/l40

Genovali, K., Lemasle, B., Bono, G., Romaniello, M., Fabrizio, M., Ferraro, I., et al. (2014). On the fine structure of the Cepheid metallicity gradient in the Galactic thin disk. *Astronomy Astrophysics* 566, A37. [astro-ph.GA]. doi:10.1051/0004-6361/201323198

Gonzalez, G., and George, W. (2000). Elemental abundances in evolved supergiants. II. The young clusters [CLC]h[/CLC] and χ persei. *Astronomical J.* 119 (4), 1839–1847. doi:10.1086/301319

Gozha, M. L., Borkova, T. V., and Marsakov, V. A. (2012). Heterogeneity of the population of open star clusters in the Galaxy. *Astron. Lett.* 38 (8), 506–518. [astro-ph.GA]. doi:10.1134/s1063773712070018

Gratton, R. G., and Contarini, G. (1994). Elemental abundances in the old open clusters NGC 2243 and Melotte 66. *Astronomy Astrophysics* 283, 911–918.

Hasegawa, T., Sakamoto, T., and Luthfi Malasan, H. (2008). New photometric data of old open clusters II. A dataset for 36 clusters. *Publ. ASJ* 60, 1267–1284. doi:10.1093/pasj/60.6.1267

Haywood, M., Di Matteo, P., Lehnert, M. D., Katz, D., and Gómez, A. (2013). The age structure of stellar populations in the solar vicinity. Clues of a two-phase formation history of the Milky Way disk. *Astronomy Astrophysics* 560, A109. [astro-ph.GA]. doi:10.1051/0004-6361/201321397

Hill, V., and Pasquini, L. (1999). A Super Lithium Rich giant in the metal-poor open cluster Berkeley 21. *Astronomy Astrophysics* 348, L21–L24. doi:10.48550/arXiv.astro-ph/9907106

Jacobson, H. R., and Eileen, D. F. (2013). Zirconium, barium, lanthanum, and europium abundances in open clusters. *Astronomical J.* 145 (4), 107. [astro-ph.GA]. doi:10.1088/0004-6256/145/4/107

Jacobson, H. R., Friel, E. D., Jílková, L., Magrini, L., Bragaglia, A., Vallenari, A., et al. (2016). The Gaia-ESO Survey: probes of the inner disk abundance gradient. *Astronomy Astrophysics* 591, A37. [astro-ph.GA]. doi:10.1051/0004-6361/201527654

Jacobson, H. R., Friel, E. D., and Pilachowski, C. A. (2008). Abundances of red giants in old open clusters. III. NGC 7142. *Astronomical J.* 135 (6), 2341–2349. doi:10.1088/0004-6256/135/6/2341

Joshi, Y. C., Dambis, A. K., Pandey, A. K., and Joshi, S. (2016). Study of open clusters within 1.8 kpc and understanding the Galactic structure. *Astronomy Astrophysics* 593, A116. [astro-ph.GA]. doi:10.1051/0004-6361/201628944

Joshi, Y. C., and Malhotra, S. (2023). Revisiting galactic disk and spiral arms using open clusters. *Astronomical J.* 166 (4), 170. [astro-ph.GA]. doi:10.3847/1538-3881/acf7c8

Just, A., and Jahreiß, H. (2010). Towards a fully consistent Milky Way disc model - I. The local model based on kinematic and photometric data. *Mon. Notices RAS* 402 (1), 461–478. [astro-ph.GA]. doi:10.1111/j.1365-2966.2009.15893.x

Kharchenko, N. V., Piskunov, A. E., Schilbach, E., Röser, S., and Scholz, R. D. (2013). Global survey of star clusters in the Milky Way: II. The catalogue of basic parameters ⋆. *Astronomy Astrophysics* 558, A53. [astro-ph.GA]. doi:10.1051/0004-6361/201322302

Krisciunas, K., Monteiro, H., and Dias, W. (2015). CCD photometry of NGC 2482 and five previously unobserved open star clusters. *Publ. ASP* 127 (947), 31–50. [astro-ph.SR]. doi:10.1086/679743

Lemasle, B., François, P., Piersimoni, A., Pedicelli, S., Bono, G., Laney, C. D., et al. (2008). Galactic abundance gradients from Cepheids: on the iron abundance gradient around 10–12 kpc. *Astronomy Astrophysics* 490 (2), 613–623. [astro-ph]. doi:10.1051/0004-6361/200810192

Lépine, J. R. D., Cruz, P., Scarano Jr, S., Barros, D. A., Dias, W. S., Pompéia, L., et al. (2011). Overlapping abundance gradients and azimuthal gradients related to the spiral structure of the Galaxy. *Mon. Notices RAS* 417 (1), 698–708. [astro-ph.GA]. doi:10.1111/j.1365-2966.2011.19314.x

Luck, R. E. (1994). Open cluster chemical composition. 1: later type stars in eight clusters. *Astrophysical J.* 91, 309. doi:10.1086/191940

Luck, R. E., Andrievsky, S. M., Kovtyukh, V. V., Gieren, W., and Graczyk, D. (2011). The distribution of the elements in the galactic disk. II. Azimuthal and radial variation in abundances from cepheids. *Astronomical J.* 142 (2), 51. [astro-ph.GA]. doi:10.1088/0004-6256/142/2/51

Maciel, W. J., and Costa, R. D. D. (2009). Abundance gradients in the galactic disk: space and time variations. https://arxiv.org/abs/0806.3443.

Maciel, W. J., Costa, R. D. D., and Idiart, T. E. P. (2010). Age distribution of the central stars of galactic disk planetary nebulae. *Astronomy Astrophysics* 512, A19. [astro-ph.GA]. doi:10.1051/0004-6361/200912499

Maciel, W. J., Lago, L. G., and Costa, R. D. D. (2005). An estimate of the time variation of the abundance gradient from planetary nebulae. II. Comparison with open clusters, cepheids and young objects. *Astronomy Astrophysics* 433 (1), 127–135. [astro-ph]. doi:10.1051/0004-6361/20042171

Magrini, L., et al. (2018). The Gaia-ESO Survey: the origin and evolution of s-process elements. *Astronomy Astrophysics* 617, A106. [astro-ph.GA]. doi:10.1051/0004-6361/201832841

Magrini, L., Randich, S., Donati, P., Bragaglia, A., Adibekyan, V., Romano, D., et al. (2015). The Gaia-ESO Survey: insights into the inner-disc evolution from open clusters. *Astronomy Astrophysics* 580, A85. [astro-ph.GA]. doi:10.1051/0004-6361/201526305

Magrini, L., Randich, S., Kordopatis, G., Prantzos, N., Romano, D., Chieffi, A., et al. (2017). The Gaia-ESO Survey: radial distribution of abundances in the Galactic disc from open clusters and young-field stars. *Astronomy Astrophysics* 603, A2. [astro-ph.GA]. doi:10.1051/0004-6361/201630294

Magrini, L., Randich, S., Zoccali, M., Jilkova, L., Carraro, G., Galli, D., et al. (2010). Open clusters towards the Galactic centre: chemistry and dynamics: a VLT spectroscopic study of NGC 6192, NGC 6404, NGC 6583⋆⋆⋆. *Astronomy Astrophysics* 523, A11. [astro-ph.GA]. doi:10.1051/0004-6361/201015395

Magrini, L., Sestito, P., Randich, S., and Galli, D. (2009). The evolution of the Galactic metallicity gradient from high-resolution spectroscopy of open clusters. *Astronomy Astrophysics* 494 (1), 95–108. [astro-ph]. doi:10.1051/0004-6361/200810634

Magrini, L., Viscasillas Vázquez, C., Spina, L., Randich, S., Romano, D., Franciosini, E., et al. (2023). The Gaia-ESO survey: mapping the shape and evolution of the radial abundance gradients with open clusters. *Astronomy Astrophysics* 669, A119. [astro-ph.GA]. doi:10.1051/0004-6361/202244957

Majewski, S. R., et al. (2017). The Apache point observatory galactic evolution experiment (APOGEE). *Astronomical J.* 154 (3), 94. [astro-ph.IM]. doi:10.3847/1538-3881/aa784d

Margheim, S. J., et al. (2000). "WIYN open cluster study: metallicity of NGC 2451," in American Astronomical Society Meeting Abstracts, Rochester, New York, USA, June, 200.

Marsakov, V. A., and Borkova, T. V. (2005). Formation of galactic subsystems in light of the magnesium abundance in field stars: the thick disk. *Astron. Lett.* 31 (8), 515–527. [astro-ph]. doi:10.1134/1.2007028

Marsakov, V. A., and Borkova, T. V. (2006). Formation of galactic subsystems in light of the magnesium abundance in field stars: the thin disk. *Astron. Lett.* 32 (6), 376–392. [astro-ph]. doi:10.1134/s1063773706060028

Martell, S. L., Sharma, S., Buder, S., Duong, L., Schlesinger, K. J., Simpson, J., et al. (2017). The GALAH survey: observational overview and Gaia DR1 companion. *Mon. Notices RAS* 465 (3), 3203–3219. [astro-ph.IM]. doi:10.1093/mnras/stw2835

Matteucci, F. (2021). Modelling the chemical evolution of the Milky way. *Astronomy Astrophysics Rev.* 29 (1), 5. [astro-ph.GA]. doi:10.1007/s00159-021-00133-8

Minchev, I., Anders, F., Recio-Blanco, A., Chiappini, C., de Laverny, P., Queiroz, A., et al. (2018). Estimating stellar birth radii and the time evolution of Milky Way's ISM metallicity gradient. *Mon. Notices RAS* 481 (2), 1645–1657. [astro-ph.GA]. doi:10.1093/mnras/sty2033

Minchev, I., Chiappini, C., and Martig, M. (2014). Chemodynamical evolution of the Milky Way disk: II. Variations with Galactic radius and height above the disk plane⋆. *Astronomy Astrophysics* 572, A92. [astro-ph.GA]. doi:10.1051/0004-6361/201423487

Monroe, T. W. R., and Catherine, A. P. (2010). Metallicities of young open clusters. I. NGC 7160 and NGC 2232". *Astronomical J.* 140 (6), 2109–2123. [astro-ph.SR]. doi:10.1088/0004-6256/140/6/2109

Mott, A., Spitoni, E., and Matteucci, F. (2013). Abundance gradients in spiral discs: is the gradient inversion at high redshift real? *Mon. Notices RAS* 435 (4), 2918–2930. [astro-ph.GA]. doi:10.1093/mnras/stt1495

Myers, N., Donor, J., Spoo, T., Frinchaboy, P. M., Cunha, K., Price-Whelan, A. M., et al. (2022a). The open cluster chemical abundances and mapping survey. VI. Galactic chemical gradient analysis from APOGEE DR17. *Astronomical J.* 164 (3), 85. [astro-ph.GA]. doi:10.3847/1538-3881/ac7ce5

Myers, N., Donor, J., Spoo, T., Frinchaboy, P. M., Cunha, K., Price-Whelan, A. M., et al. (2022b). The open cluster chemical abundances and mapping survey. VI. Galactic chemical gradient analysis from APOGEE DR17. *Astronomical J.* 164 (3), 85. [astro-ph.GA]. doi:10.3847/1538-3881/ac7ce5

Netopil, M., Oralhan, İ. A., Çakmak, H., Michel, R., and Karataş, Y. (2022). The Galactic metallicity gradient shown by open clusters in the light of radial migration. *Mon. Notices RAS* 509 (1), 421–439. [astro-ph.GA]. doi:10.1093/mnras/stab2961

Netopil, M., and Paunzen, E. (2013). Towards a photometric metallicity scale for open clusters. *Astronomy Astrophysics* 557, A10. [astro-ph.SR]. doi:10.1051/0004-6361/201321829

Netopil, M., Paunzen, E., Heiter, U., and Soubiran, C. (2016). On the metallicity of open clusters. III. Homogenised sample. *Astronomy Astrophysics* 585, A150. [astro-ph.SR]. doi:10.1051/0004-6361/201526370

Overbeek, J. C., Friel, E. D., and Heather, R. J. (2016). New neutron-capture measurements in 23 open clusters. I. The r-process. *Astrophysical J.* 824 (2), 75. [astro-ph.SR]. doi:10.3847/0004-637x/824/2/75

Pancino, E., Carrera, R., Rossetti, E., and Gallart, C. (2010). Chemical abundance analysis of the open clusters Cr 110, NGC 2099 (M 37), NGC 2420, NGC 7789, and M 67 (NGC 2682). *Astronomy Astrophysics* 511, A56. [astro-ph.GA]. doi:10.1051/0004-6361/200912965

Pasquini, L., Randich, S., Zoccali, M., Hill, V., Charbonnel, C., and Nordström, B. (2004). Detailed chemical composition of the open cluster IC 4651: the iron peak, elements, and Li. *Astronomy Astrophysics* 424, 951–963. [astro-ph]. doi:10.1051/0004-6361:20040240

Paunzen, E., Heiter, U., Netopil, M., and Soubiran, C. (2010). On the metallicity of open clusters. I. Photometry. *Astronomy Astrophysics* 517, A32. doi:10.1051/0004-6361/201014131

Paunzen, E., Maitzen, H. M., Rakos, K. D., and Schombert, J. (2003). Strömgren uvby photometry of the open clusters NGC 6192 and NGC 6451. *Astronomy Astrophysics* 403, 937–941. [astro-ph]. doi:10.1051/0004-6361:20030443

Pereira, C. B., and Quireza, C. (2010). "Abundances of seven red giants in the open cluster NGC 3114". In: *Star clusters: basic galactic building blocks throughout time and space.* Ed. by de G. Richard, and R. D. L. Jacques, International Astronomical Union, Paris, France, doi:10.1017/S1743921309991803

Piatti, A. E., Claria, J. J., and Abadi, M. G. (1995). Chemical evolution of the galactic disk: evidence for a gradient perpendicular to the galactic plane. *Astronomical J.* 110, 2813. doi:10.1086/117731

Piecka, M., and Paunzen, E. (2021). Aggregates of clusters in the Gaia data. *Astronomy Astrophysics* 649, A54. [astro-ph.IM]. doi:10.1051/0004-6361/202040139

Prantzos, N., and Aubert, O. (1995). On the chemical evolution of the galactic disk. *Astronomy Astrophysics* 302, 69.

Randich, S., et al. (2022). The Gaia-ESO Public Spectroscopic Survey: implementation, data products, open cluster survey, science, and legacy. *Astronomy Astrophysics* 666, A121. [astro-ph.GA]. doi:10.1051/0004-6361/202243141

Reddy, A. B. S., Giridhar, S., and Lambert, D. L. (2013). Comprehensive abundance analysis of red giants in the open clusters NGC 2527, 2682, 2482, 2539, 2335, 2251 and 2266. *Mon. Notices RAS* 431 (4), 3338–3348. [astro-ph.GA]. doi:10.1093/mnras/stt412

Reddy, A. B. S., Giridhar, S., and Lambert, D. L. (2020). Galactic chemical evolution and chemical tagging with open clusters. *J. Astrophysics Astronomy* 41 (1), 38. doi:10.1007/s12036-020-09658-3

Reddy, A. B. S., Lambert, D. L., and Giridhar, S. (2016). The evolution of the Milky Way: new insights from open clusters. *Mon. Notices RAS* 463 (4), 4366–4382. [astro-ph.GA]. doi:10.1093/mnras/stw2287

Reddy, B. E., Tomkin, J., Lambert, D. L., and Prieto, C. A. (2003). The chemical compositions of Galactic disc F and G dwarfs. *Mon. Notices RAS* 340 (1), 304–340. doi:10.1046/j.1365-8711.2003.06305.x

Reid, M. J., Menten, K. M., Brunthaler, A., Zheng, X. W., Dame, T. M., Xu, Y., et al. (2019). Trigonometric parallaxes of high-mass star-forming regions: our view of the Milky way. *Astrophysical J.* 885 (2), 131. [astro-ph.GA]. doi:10.3847/1538-4357/ab4a11

Rix, H.-W., and Jo, B. (2013). The Milky Way's stellar disk. Mapping and modeling the Galactic disk. *Astronomy Astrophysics Rev.* 21, 61. [astro-ph.GA]. doi:10.1007/s00159-013-0061-8

Santos, N. C., Lovis, C., Melendez, J., Montalto, M., Naef, D., and Pace, G. (2012). Metallicities for six nearby open clusters from high-resolution spectra of giant stars. [Fe/H] values for a planet search sample. *Astronomy Astrophysics* 538, A151. [astro-ph]. doi:10.1051/0004-6361/201118276

Santos, N. C., Lovis, C., Pace, G., Melendez, J., and Naef, D. (2009). Metallicities for 13 nearby open clusters from high-resolution spectroscopy of dwarf and giant stars. Stellar metallicity, stellar mass, and giant planets. *Astronomy Astrophysics* 493 (1), 309–316. [astro-ph]. doi:10.1051/0004-6361:200811093

Schlesinger, K. J., Johnson, J. A., Rockosi, C. M., Lee, Y. S., Beers, T. C., Harding, P., et al. (2014). The vertical metallicity gradient of the Milky way disk: transitions in [α/Fe] populations. *Astrophysical J.* 791 (2), 112. [astro-ph.GA]. doi:10.1088/0004-637x/791/2/112

Schuler, S. C., King, J. R., Fischer, D. A., Soderblom, D. R., and Jones, B. F. (2003). Spectroscopic abundances of solar-type dwarfs in the open cluster M34 (NGC 1039). *Astronomical J.* 125 (4), 2085–2097. doi:10.1086/373927

Sestito, P., Randich, S., Mermilliod, J. C., and Pallavicini, R. (2003). The evolution of lithium depletion in young open clusters: NGC 6475. *Astronomy Astrophysics* 407, 289–301. [astro-ph]. doi:10.1051/0004-6361:20030723

Soubiran, C., Bienaymé, O., Mishenina, T. V., and Kovtyukh, V. V. (2008). Vertical distribution of Galactic disk stars. IV. AMR and AVR from clump giants. *Astronomy Astrophysics* 480 (1), 91–101. [astro-ph]. doi:10.1051/0004-6361:20078788

Spina, L., Magrini, L., and Cunha, K. (2022). Mapping the galactic metallicity gradient with open clusters: the state-of-the-art and future challenges. *Universe 8.2* 8, 87. [astro-ph.GA]. doi:10.3390/universe8020087

Spina, L., Randich, S., Magrini, L., Jeffries, R. D., Friel, E. D., Sacco, G. G., et al. (2017). The Gaia-ESO Survey: the present-day radial metallicity distribution of the Galactic disc probed by pre-main-sequence clusters. *Astronomy Astrophysics* 601, A70. [astro-ph.SR]. doi:10.1051/0004-6361/201630078

Spina, L., Ting, Y. S., De Silva, G. M., Frankel, N., Sharma, S., Cantat-Gaudin, T., et al. (2021). The GALAH survey: tracing the Galactic disc with open clusters. *Mon. Notices RAS* 503 (3), 3279–3296. [astro-ph.GA]. doi:10.1093/mnras/stab471

Toyouchi, D., and Masashi, C. (2014). On the chemical and structural evolution of the galactic disk. *Astrophysical J.* 788 (1), 89. [astro-ph.GA]. doi:10.1088/0004-637x/788/1/89

Twarog, B. A., Ashman, K. M., and Barbara, J.A.-T. (1997). Some revised observational constraints on the formation and evolution of the galactic disk. *Astronomical J.* 114, 2556. [astro-ph]. doi:10.1086/118667

Vansevicius, V., Platais, I., Paupers, O., and Abolins, E. (1997). A study of the open cluster NGC 7209 in the Vilnius photometric system. *Mon. Notices RAS* 285 (4), 871–878. doi:10.1093/mnras/285.4.871

Vickers, J. J., Juntai, S., and Zhao-Yu, Li. (2021). The flattening metallicity gradient in the Milky way's thin disk. *Astrophysical J.* 922 (2), 189. [astro-ph.GA]. doi:10.3847/1538-4357/ac27a9

Villanova, S., Carraro, G., Bresolin, F., and Patat, F. (2005). Metal abundances in extremely distant galactic old open clusters. II. Berkeley 22 and Berkeley 66. *Astronomical J.* 130 (2), 652–658. [astro-ph]. doi:10.1086/430958

Vincenzo, F., Kobayashi, C., and Taylor, P. (2018). On the [α/Fe]-[Fe/H] relations in early-type galaxies. *Mon. Notices RAS* 480 (1), L38–L42. [astro-ph.GA]. doi:10.1093/mnrasl/sly128

Viscasillas Vázquez, C., Magrini, L., Casali, G., Tautvaišienė, G., Spina, L., Van der Swaelmen, M., et al. (2022). The Gaia-ESO survey: age-chemical-clock relations spatially resolved in the Galactic disc. *Astronomy Astrophysics* 660, A135. [astro-ph.GA]. doi:10.1051/0004-6361/202142937

Warren, S. R., and Cole, A. A. (2009). Metallicities and radial velocities of five open clusters including a new candidate member of the Monoceros stream ∗. *Mon. Notices RAS* 393 (1), 272–296. [astro-ph]. doi:10.1111/j.1365-2966.2008.14268.x

Wu, Z.-Yu, Zhou, X., Ma, J., and Du, C. H. (2009). The orbits of open clusters in the Galaxy. *Mon. Notices RAS* 399 (4), 2146–2164. [astro-ph.GA]. doi:10.1111/j.1365-2966.2009.15416.x

Wyse, R. F. G. (1999). Chemical evolution of the galactic disk and bulge. *Astronomy Astrophysics* 267, 145–166. [astro-ph]. doi:10.1023/a:1002796330242

Yong, D., Carney, B. W., and Friel, E. D. (2012a). Elemental abundance ratios in stars of the outer galactic disk. IV. A new sample of open clusters. *Astronomical J.* 144 (4), 95. [astro-ph.GA]. doi:10.1088/0004-6256/144/4/95

Yong, D., Carney, B. W., and Friel, E. D. (2012b). Elemental abundance ratios in stars of the outer galactic disk. IV. A new sample of open clusters. *Astronomical J.* 144 (4), 95. [astro-ph.GA]. doi:10.1088/0004-6256/144/4/95

Začs, L., Alksnis, O., Barzdis, A., Laure, A., Musaev, F. A., Bondar, A., et al. (2011). Spectroscopy of red giants in the open clusters NGC 1545 and Tr2. *Mon. Notices RAS* 417 (1), 649–658. doi:10.1111/j.1365-2966.2011.19309.x

Zhang, H., Chen, Y., and Zhao, G. (2021). Radial migration from the metallicity gradient of open clusters and outliers. *Astrophysical J.* 919 (1), 52. [astro-ph.GA]. doi:10.3847/1538-4357/ac0e92

Zhong, J., Chen, L., Wu, D., Li, L., Bai, L., and Hou, J. (2020). Exploring open cluster properties with Gaia and LAMOST. *Astronomy Astrophysics* 640, A127. [astro-ph.GA]. doi:10.1051/0004-6361/201937131